Supporting Information for

Cross-bridged cyclam derivatives with bis(phosphinate) and phosphinate-phosphonate pendant arms (cb-BPC) as chelators for copper radioisotopes

Peter Urbanovský,[a] Tomáš David,[a,b #] Veronika Hlinová,[a] Vojtěch Kubíček,[a] Hans-Jürgen Pietzsch,[b] Petr Hermann[a]*

[a]Department of Inorganic Chemistry, Faculty of Science, Charles University, Hlavova 2030/8, 128 00 Prague 2, Czechia. *E-mail: petrh@natur.cuni.cz ; Tel.: +420 221921263.

[b]Institute of Radiopharmaceutical Cancer Research, Helmholtz-Zentrum Dresden-Rossendorf, Bautzner Landstrasse 400, 013 28 Dresden, Germany.

[#]Current address: Institute of Organic Chemistry and Biochemistry (IOCB), Academy of Science of the Czech Republic, Flemingovo náměstí 542/2, 160 00 Prague 6, Czechia.

Content: Page

Simplified synthesis of cross-bridged cyclam (cb-cyclam).

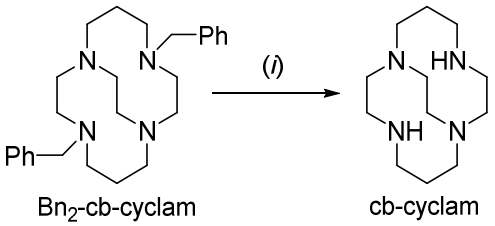

(*i*) Pd/C (10 % w/w), H_2 (1 atm.), 90% aq. AcOH, 50 °C, 2 d.

The Bn_2-cb-cyclam was prepared by the published procedure[1] and its deprotection was simplified.

Compound Bn_2-cb-cyclam (2.1 g, 5.1 mmol) and Pd/C (0.21 g, 10 % w/w) were suspended in 90 % aq. AcOH (100 ml) and the flask was well flushed with hydrogen gas and a hydrogen balloon was attached. The mixture was vigorously stirred and heated to 50 °C for 2 d. The solids were filtered off through a syringe microfilter (0.22 μm) and solvents were removed *in vacuo*. The oily residue was co-evaporated with toluene (2×10 ml) and then re-dissolved in THF (100 ml). To this vigorously stirred solution, a mixture of Me_3Si-Cl (3.1 ml, 5 equiv.) and *i*PrOH (1.8 ml, 5 equiv.) in dry Et_2O (20 ml) was added in one portion. The product precipitated as a white powder. Sonification helped to break up the precipitate into "smaller" particles. The solids were filtered off on a fine frit under a semi-inert filtration (*i.e.* dry N_2 gas stream was gently blew through a glass funnel inversely placed just over the glass frit with the product), washed with dry Et_2O (3×25 ml) and dried under dry N_2. The cross-bridged cyclam was isolated as dihydrochloride (1.9 g, >90 % as off-white hygroscopic powder) which was stored in a desiccator over P_2O_5.

Caution! The cb-cyclam as a free base is extremely hydroscopic and quickly absorbs CO_2 from air, both as a solid or in solution. The hydrochloride is much easier to handle with.

Synthesis of phthalimido-*N*-methylcarbaldehyde (PhthN–CH_2–CHO).

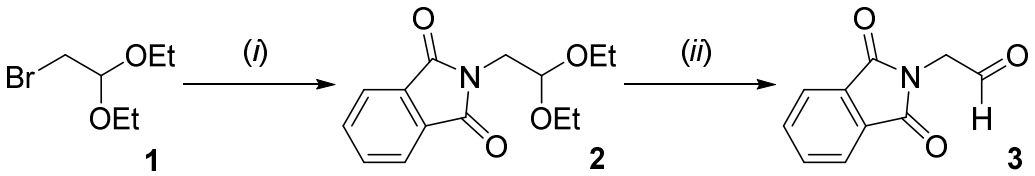

(*i*) potassium phthalimide (1 equiv.), DMF, 150 °C, 1 d. (*ii*) TFA:$CHCl_3$ ~1:1, room temperature, overnight.

Compound **1** (8.3 ml, 54 mmol, 1 equiv.) and potassium phthalimide (10.0 g, 54 mmol, 1 equiv.) were mixed with DMF (200 ml), and the mixture were stirred and heated to 150 °C for 1 d. The solution was cooled to room temperature and poured into water (400 ml). The suspension was left in a fridge for 1 d. Then, the crystalline solid was filtered off on a fine frit and dried in a desiccator over P_2O_5. Compound **2** (12.2 g, 86 %) was isolated as a brown solid. The spectral data were identical to those published.[2]

Compound **2** (7.0 g, 26.6 mmol) was dissolved in a mixture of TFA:$CHCl_3$ 1:1 *v*/*v* (100 ml) and the solution was stirred at room temperature overnight. Then, volatiles were removed in vacuum and the residue was co-evaporated

[1] E. H. Wong, G. R. Weisman, D. C. Hill, D. P. Reed, M. E. Rogers, J. S. Condon, M. A. Fagan, J. C. Calabrese, K.-C. Lam, I. A. Guzei, A. L. Rheingold, *J. Am. Chem. Soc.* **2000,** *122*, 10561–10572.

[2] Y. Pérez-Otero, M. I. Fernández-García, E. Gómez-Fórneas, G. González-Riopedre, M. Maneiro, *J. Chem.* **2015**, 963152.

with toluene (10 ml). The residue was triturated with *n*-hexane (50 ml) using sonification. The solid was filtered off on a fine frit, washed with *n*-hexane (2×10 ml) and dried on air. Compound **3** was isolated as brownish powder (4.8 g, 95 %). The spectral data were identical to those published.[2]

Modified synthesis of (4-NO_2-benzyl)(OH)(O)P–CH_2–P(O)(OH)(H) (compound C).

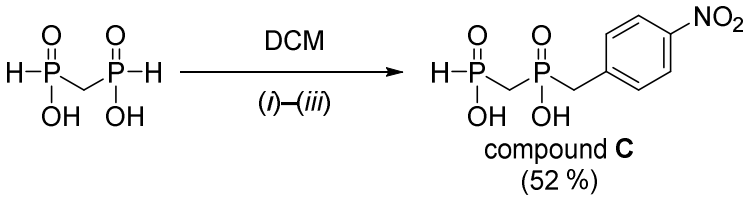

(*i*) TMSCl (4 equiv.), BSA (2 equiv.), DIPEA (8 equiv.), anhydrous DCM, Ar atmosphere, 0 °C → room temperature, 1 h; (*ii*) 4-NO_2BnBr (1.2 equiv.), anhydrous DCM, Ar atmosphere, room temperature, 3 d; (*iii*) EtOH (excess), 0 °C → room temperature, 10 min.

In 500-ml three-necked round-bottom flask, solid methylene-bis(*H*-phosphinic acid) **A** (~4.8 g, 33 mmol, 1 equiv.) was flushed with argon. Under the argon atmosphere, anhydrous DCM (100 ml) and DIPEA (~48 ml, 267 mmol, 8 equiv.) were added *via* a syringe. The mixture was cooled in an ice bath and TMS-Cl (~17 ml, 133 mmol, 4 equiv.) and BSA (16.3 ml, 67 mmol, 2 equiv.) were consecutively added *via* syringe. The mixture was left to heat to room temperature during ~1 h and 4-nitrobenzyl bromide (4-NO_2BnBr, 9.1 g, 40 mmol, 1.2 equiv.) dissolved in anhydrous DCM (~50 ml) was added *via* a syringe under Ar atmosphere. The mixture was stirred at room temperature under Ar atmosphere for 3 d. Then, the solution was cooled in an ice bath and EtOH (~25 ml) was carefully added *via* a syringe. After stirring for 10 min, water (~50 ml) was added to the solution and the mixture was evaporated to dryness at reduced pressure. The residue was co-evaporated with toluene (2 × 20 ml) and with water (~50 ml). The oily residue was dissolved in water (~20 ml) and the solution was poured onto a strong cation exchanger (Dowex 50, ~5×20 cm, H^+-form). The crude product was then eluted off with ~20% aq. EtOH. Solvents were removed at reduced pressure and the oily residue was suspended in water (~50 ml). The suspension was filtered through a glass frit (S4) and the filtrate was concentrated at reduced pressure. The concentrated solution was poured onto a weak cation exchanger (Amberlite CG50, ~5×15 cm, H^+-form) and the column was washed with water. The fractions (~25 ml) containing the product (checked by TLC (conc. aq. NH_3 : EtOH ~1:5): R_f 0.5) were combined and concentrated at reduced pressure. The residue was dissolved in THF (100 ml) and the solution was put into a fridge. After 1 d, the crystalline **C** was filtered off (S3). The crystals were washed with Et_2O (3× 25 ml) and dried on air. Compound **C** was obtained as white hemihydrate (4.9 g, 52 %) and was stored in a dark place. Elemental analysis (calc. for $C_8H_{11}NO_7P_2 \cdot 0.5H_2O$, M_R 304.0): C 33.2 (33.4), H 3.8 (4.2), N 5.2 (4.9). HR-MS (calc. for $[C_8H_{10}O_7NP_2]^+$): 293.99353 (293.99380). The other characterization data were identical to those published.[3]

[3] T. David, V. Hlinová, V. Kubíček, R. Bergmann, F. Striese, N. Berndt, D. Szöllősi, T. Kovács, D. Máthé, M. Bachmann, H.-J. Pietzsch, P. Hermann, *J. Med. Chem.* **2018**, *61*, 8774–8796.

Table S1

Gradients used in analytical and semi-preparative HPLC, and in automated flash chromatography.

Semi-preparative (analytical in parentheses) HPLC* and flash chromatography[&]			
Method number	Linear gradient of A:B:C	Time of gradient, min	Flow rate, ml/min
M1	85:10:5 → 0:10:90	11.4 (5)	15.0 (1.0)
M2	0:100:0 → 0:100:0 → 0:0:100 → 0:0:100	5+18+3 (2+6+3)	12.0 (1.2)
M3	55:40:5 → 20:40:40	70 (30)	15.0 (1.0)
M4	0:90:10 → 0:90:10 → 0:70:30	2+25	12.0
M5	0:95:5 → 0:50:50	50	12.0
M6	0:100:0 → 0:100:0 → 0:70:30	2+30	12.0
M7	70:30:0 → 70:30:0 → 30:70:0 → 0:100:0	3+15+3	12.0

*****A = water, B = 0.1 % aq. TFA, C = MeCN. Detection at 210 and 254 nm.

[&]A = water, B = 0.1 % aq. HCl, C = MeCN. Detection at 215, 254, and 284 nm; flow rate 50 ml/min.

Figure S1.

Structure of the ditopic "**bis-1**" by-product.

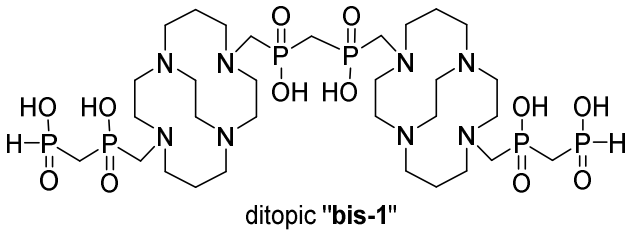

Figure S2.

A typical $^{31}P\{^{1}H\}$ NMR spectrum of *in situ* reaction mixture obtained after heating **11**, DIPEA, BSA and $Me_3Si–Cl$ in anhydrous $CHCl_3$ at 50 °C for ~60 min (Scheme 3 in the main text). The signal at ~150–155 ppm corresponds to the trivalent $R–P^{III}(OTMS)_2$ moiety, the signals at 20–40 ppm correspond to the pentavalent phosphorus esters. The phosphorus atoms after esterification become chiral.

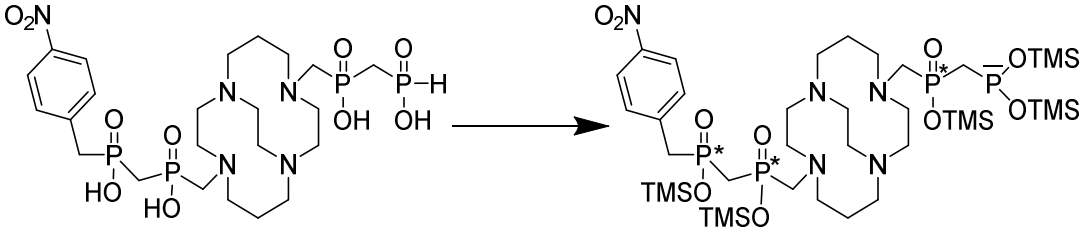

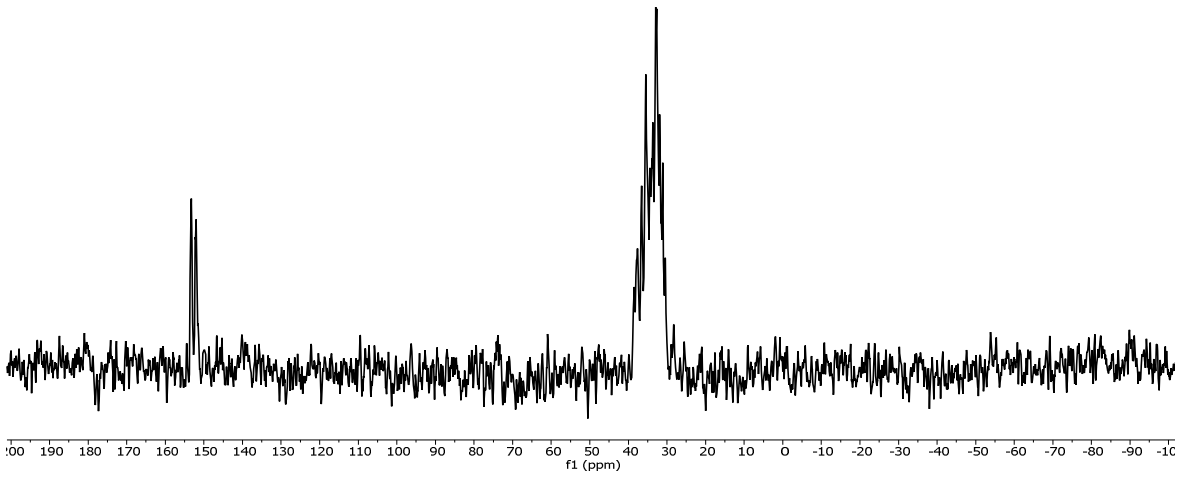

Reduction of the nitrile-containing compound 14 to compounds 24 and 24a

Reduction of nitrile group to desired amine group in **14** was not possible. Partial success was reached with common procedure involving Ra-Ni in alkaline media where desired compound **24** was obtained in a very low yield and after an extensive purification. The decomposition of the compounds and, mainly, formation of Ni(II) complexes of **8**, **14**, **24** and **24a** was observed (HPLC-MS). A buffered aq. solution (pH ~9.5 by benzylamine) was also used. It led to a highly preferential reduction of the nitro group (to **24a**) at room temperature and, at higher temperature (50 °C), the major products were Ni^{2+} complexes of **24a** and **14** (in molar ratio ~5:1) which were isolated by semi-preparative HPLC. Utilization of higher pH led to partial cleavage of pendant arm(s) of compound **14**. Hence, preparation of **24** from **14** for an additional compound derivatization was no further pursued.

Compound 24.

In a 4-ml glass vial, $NiCl_2 \cdot 6H_2O$ (4.8 mg, 20 μmol, 1 equiv.) was dissolved in water (2 ml). The $NaBH_4$ (7.6 mg, 20 μmol, 10 equiv.) was added in one portion to the solution and precipitation of dark slurry of Raney nickel was observed. The suspension was stirred at room temperature for 10 min and compound **14**·1.5TFA·$3H_2O$ (19.0 mg, 20 μmol, 1 equiv.) was added. The mixture was stirred at room temperature for 1 day. Then, another portion of $NaBH_4$ (7.6 mg, 20 μmol, 10 equiv.) was added and stirring continued for another day. Then, the solids were filtered off using a syringe PVDF microfilter (0.22 μm) and the filtrate was purified by semi-preparative HPLC (C-18, M6). Fractions with the pure compound (HPLC) were combined and lyophilized to get compound **24** as TFA salt as a clear oil (1.5 mg, ~10 %, purity ~90%, Figure S31).

NMR (D_2O, pD ~7.2): ^{1}H δ 1.69–1.86 (P–C***H***$_2$–CH_2–CH_2 + CH_2–C***H***$_2$–CH_2, bm, 4H), 1.86–1.94 (P–CH_2–C***H***$_2$–CH_2, bm, 2H), 2.02–2.18 (2× P–C***H***$_2$–P, bm, 4H), 2.18–2.37 (CH_2–C***H***$_2$–CH_2, bm, 2H), 2.60–2.84 (***cycle***, bm, 4H), 2.84–2.97 (***cycle***, bm, 4H), 2.97–3.10 (***cycle*** + P–CH_2–CH_2–C***H***$_2$ + P–C***H***$_2$–C_{aryl}, bm, 6H), 3.10–3.25 (***cycle***, bm, 2H), 3.25–3.37 (***cycle***, bm, 2H), 3.37–3.74 (***cycle*** + N–C***H***$_2$–P, bm, 12H), 6.83–6.87 (***m-phenyl***, m, 2H), 7.15–7.21 (***o-phenyl***, m, 2H); ^{13}C{^{1}H} δ 20.9 (P–CH_2–***C***H_2–CH_2, d, $^2J_{CP}$ 2.9), 21.0–21.2 (2× CH_2–***C***H_2–CH_2, bs), 29.0 (P–***C***H_2–CH_2–CH_2, d, $^1J_{CP}$ 95.6), 34.4 (P–***C***H_2–P, pseudo-t, $^1J_{CP}$ ~ $^1J_{CP}$ 82.5), 35.4 (P–***C***H_2–P, pseudo-t, $^1J_{CP}$ ~ $^1J_{CP}$ 85.9), 39.1 (P–***C***H_2–C_{aryl}, d, $^1J_{CP}$ 92.7), 40.9 (P–CH_2–CH_2–***C***H_2, d, $^3J_{CP}$ 17.2), 49.2–50.6 (***cycle***, bm), 52.6–55.2 (***cycle*** + N–***C***H_2–P, bm), 56.7–58.8 (***cycle***, bm), 117.5 (***m-phenyl***, s), 126.5–126.7 (***i-phenyl***, bm), 131.4 (***o-phenyl***, d, $^3J_{CP}$ 5.0), 144.2 (***p-phenyl***, s). ^{31}P{^{1}H} δ 21.5–26.2 (m, 2P), 32.6 (s, 1P), 34.6 (s, 1P). ESI-MS: (–) 699.3 (699.3, $[M–H]^-$), 349.1 (349.1, $[M–2H]^{2-}$); (+) 701.3 (701.3, $[M+H]^+$). ESI-HR-MS: (+) 701.28660 (701.28698, $[C_{26}H_{53}O_8N_6P_4]^+$); (–) 699.27285 (699.27243, $[C_{26}H_{51}O_8N_6P_4]^-$). HPLC (C-18, M2): R_f ~2.2 min.

Complexes Ni(II)–24a and Ni(II)–14.

In a 20-ml glass vial, $NiCl_2 \cdot 6H_2O$ (7.5 mg, 31.5 μmol, 1 equiv.) was dissolved in water (~5 ml). To this solution, $NaBH_4$ (6.0 mg, 185 μmol, 5 equiv.) was added in one portion and precipitation of dark slurry of Raney nickel was observed. After 10 min of stirring at room temperature, buffered solution (~5 ml) of compound **14**·$3H_2O$·1.5TFA (30.0 mg, 31.5 μmol, 1 equiv.) containing benzylamine (34 μl, 315 μmol, 10 equiv.) and adjusted by aq. HCl to pH 9.0 was added to the RaNi suspension. Then, another portion of $NaBH_4$ (6.0 mg, 185 μmol, 5 equiv.) was added, and the suspension was stirred at 50 °C for 1 d. Solids were filtered off using a PVDF syringe microfilter (0.22 μm) and the filtrate was concentrated under reduced pressure to ~5 ml. This solution was purified by a semi-preparative HPLC (C-

18, M6). The **Ni(II)–24a** and **Ni(II)–14** complexes (according to MS-HPLC) were obtained in a pure form and fractions containing the pure complexes were combined and directly lyophilized. Trifluoroacetate salts of Ni(II) complexes of **24a** and **14** were isolated as slightly pink fluffy solids (8.0 and 1.0 mg, respectively).

Compound **Ni(II)–24a**: ESI-MS: (+) 753.2 (753.2, $[M+H]^+$), 377.1 (377.1, $[M+2H]^{2+}$). The Ni isotope pattern was observed. HPLC (C-18, M2): R_f ~3.54 min.

Compound **Ni(II)–14**: ESI-MS: (+) 757.2 (757.2, $[M+H]^+$), 379.1 (379.1, $[M+2H]^{2+}$). The Ni isotope pattern was observed. HPLC (C-18, M2): R_f ~3.46 min.

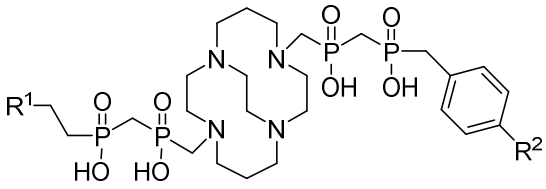

14
R^1 = CN
R^2 = NO_2

24
R^1 = CH_2NH_2
R^2 = NH_2

24a
R^1 = CN
R^2 = NH_2

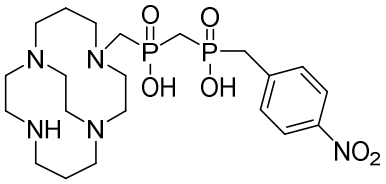

8

Figure S3

Comparison of radiolabelling efficiency of selected chelators prepared in this work with the established ones, H_4cb-te2ac and H_4cb-te2p. The H_2te1pp^H was used as a "standard" chelator (labelled as "control") to check quality of the ^{64}Cu batches.[4] Freshly prepared batches of 9–11 MBq non-carrier added (NCA) [^{64}Cu]$CuCl_2$ were used.

Conditions: pH 5.5 (0.5 M MES-NaOH buffer), ~100 equiv. of the chelators over molar amount of ^{64}Cu, room temperature, labelling time 1 h.

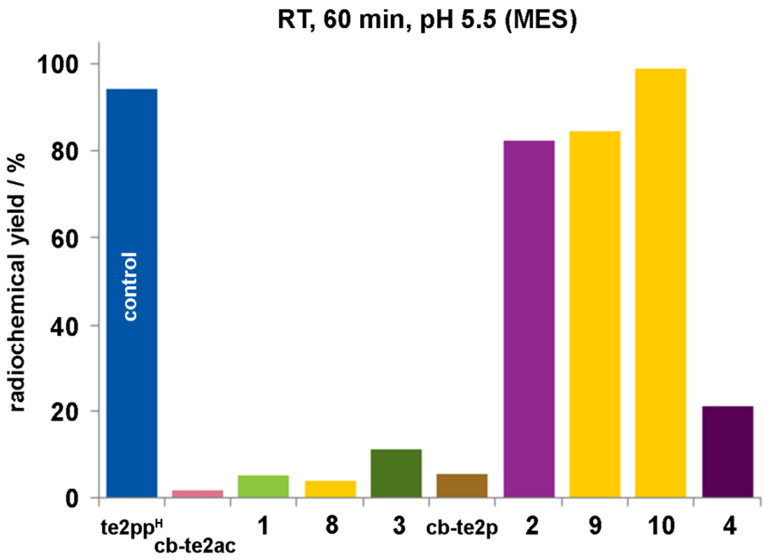

[4] T. David, V. Kubíček, O. Gutten, P. Lubal, J. Kotek, H.-J. Pietzsch, L. Rulíšek, P. Hermann, Cyclam derivatives with a bis(phosphinate) or a phosphinato-phosphonate pendant arm: ligands for fast and efficient copper(II) complexation for nuclear medical applications. *Inorg. Chem.* **2015**, *54*, 11751–11766.

Solid-state structure of compound C

The single crystal suitable for X-ray diffraction analysis was obtained on standing of the mother THF solution after crystallization of the main portion of compound **C** (see above).

The selected crystal of **C** was mounted on a glass fibre in a random orientation and the diffraction data were collected by Bruker D8 VENTURE Duo diffractometer with a micro-focus sealed tube using Mo-K_α radiation (λ 0.71073 Å) at 120 K. Data were analysed using the SAINT software package (Bruker AXS Inc., 2015–2019). Data were corrected for absorption effects using the multi-scan method (SADABS).[5] The structure was solved by direct methods (SHELXT2018)[6] and refined using full-matrix least-squares techniques (SHELXL2017).[7]

One molecule of **C** is present in the structurally independent unit. All non-hydrogen atoms were refined anisotropically. The hydrogen atoms were localised in the electron density map; however, that bound to the phosphorus atom was kept in the original position with U_{eq}(H) = 1.2 U_{eq}(P) as its refinement led to an unrealistically small thermal factor, and those bound to the carbon atoms were placed in theoretical positions using U_{eq}(H) = 1.2 U_{eq}(C) to keep the number of parameters low. Only hydrogen atoms bound to the oxygen atoms were fully refined. An overview of experimental crystallographic data is given in Table S2. Geometry around the phosphorus atoms is roughly tetrahedral. The molecules are connected by an extended system of very strong hydrogen bonds. Geometric parameters of the hydrogen bonds are listed in Table S3. The molecular structure of **C** is shown in Figure S4 and the crystal packing is shown in Figure S5.

Table S2. Experimental crystallographic data for the crystal structure of **C**.

Compound	**C**
Formula	$C_8H_{11}NO_6P_2$
M	279.12
Crystal system	monoclinic
Space group	$P2_1/c$
a / Å	13.3534(4)
b / Å	8.1042(2)
c / Å	10.3592(2)
β / °	91.772(1)
U / Å^3	1120.52(5)
Z	4
Unique refl.	2559
Obsd. refl.	2458
$R(I>2\sigma(I))$; *R'*	0.0248; 0.0258
$wR(I>2\sigma(I))$; *wR'*	0.0701; 0.0711
CCDC	2341020

[5] L. Krause, R. Herbst-Irmer, G. M. Sheldrick, D. Stalke, *J. Appl. Cryst.*, 2015, **48**, 3–10.

[6] (*a*) G. M. Sheldrick, *SHELXT2018/2. Program for Crystal Structure Solution from Diffraction Data*, University of Göttingen, Göttingen, 2014; (*b*) G. M. Sheldrick, *Acta Crystallogr. Sect. A.*, 2008, **A64**, 112–122.

[7] *a*) C. B. Hübschle, G. M. Sheldrick, B. Dittrich, *ShelXle: a Qt graphical user interface for SHELXL*, University of Göttingen, Göttingen, 2014. (*b*) C. B. Hübschle, G. M. Sheldrick, B. Dittrich, *J. Appl. Cryst.*, 2011, **44**, 1281–1284. (*c*) G. M. Sheldrick, *Acta Crystallogr. Sect. C*, 2015, **C71**, 3–8. (*d*) G. M. Sheldrick, *SHELXL-2017/1. Program for Crystal Structure Refinement from Diffraction Data*, University of Göttingen, Göttingen, 2017.

Table S3. Geometric parameters of hydrogen bonds found in the crystal structure of **C**.

D–H	*d*(D–H) / Å	*d*(H···A) / Å	<DHA / °	*d*(D···A) / Å	A
O11–H11O	0.86(2)	1.61(3)	177(3)	2.473(1)	O22 [−*x*+1, *y*−1/2, −*z*+3/2]
O21–H21O	0.82(2)	1.66(2)	172(2)	2.484(1)	O12 [−*x*+1, −*y*+2, −*z*+1]

Figure S4. Molecular structure of unsymmetrical methylene-bis(phosphinic acid) **C**.

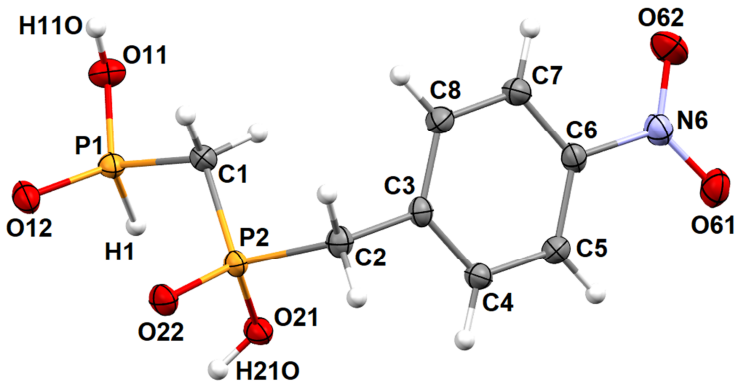

Figure S5. Hydrogen bond system found in the crystal structure of **C**. Hydrogen bonds connecting molecules are turquoise, those pointing to further molecules are shown in magenta; only the hydrogen/oxygen atoms of the other molecule are shown. Atom labels a–i are used to distinguish different symmetry-related molecules.

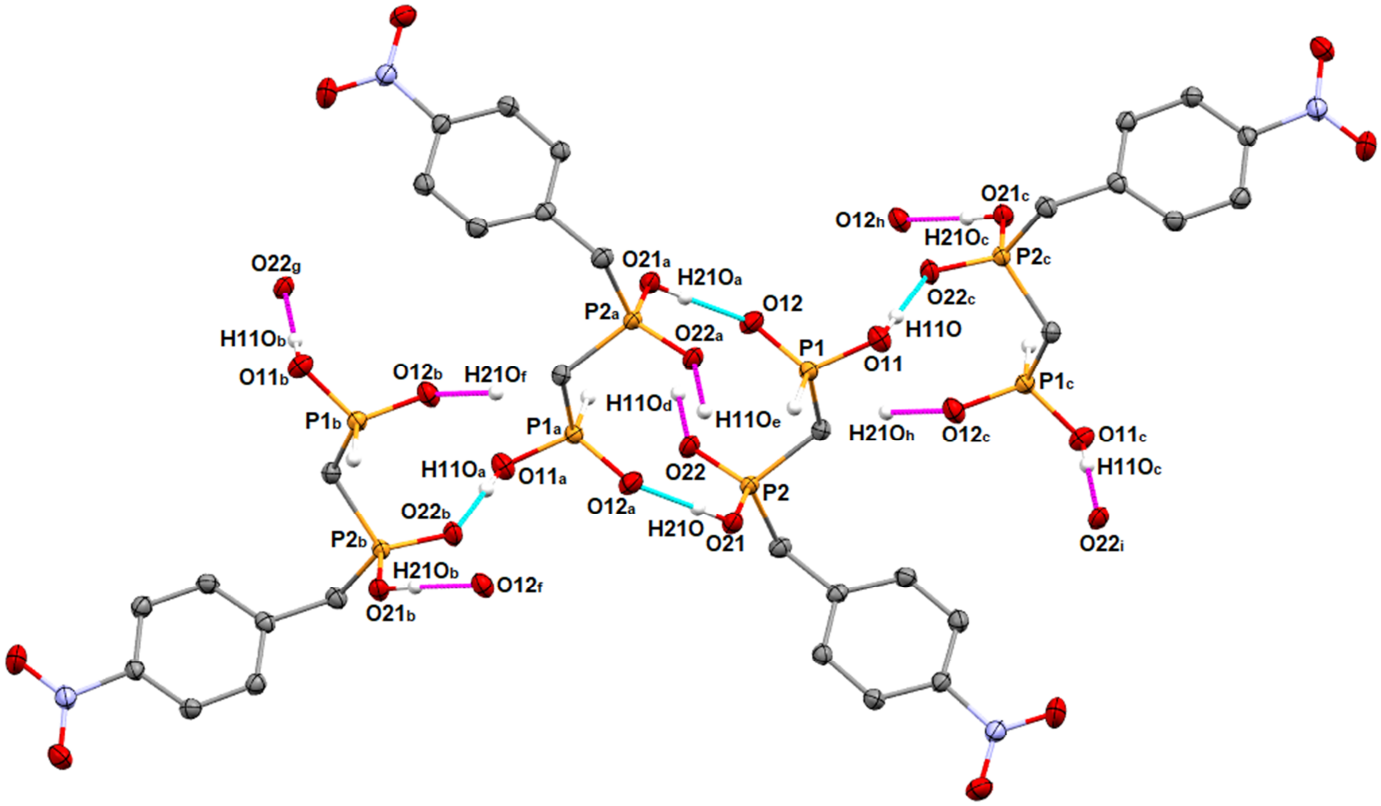

Figure S6. Characterization ^{31}P (**A**), ^{1}H (**B**) and $^{13}C\{^{1}H\}$ (**C**) NMR spectra of methylene-(*H*-phosphinic-phosphonic acid) **B** in H_2O+LiOH (pH ≥12). Signals of *t*-BuOH were labelled *.

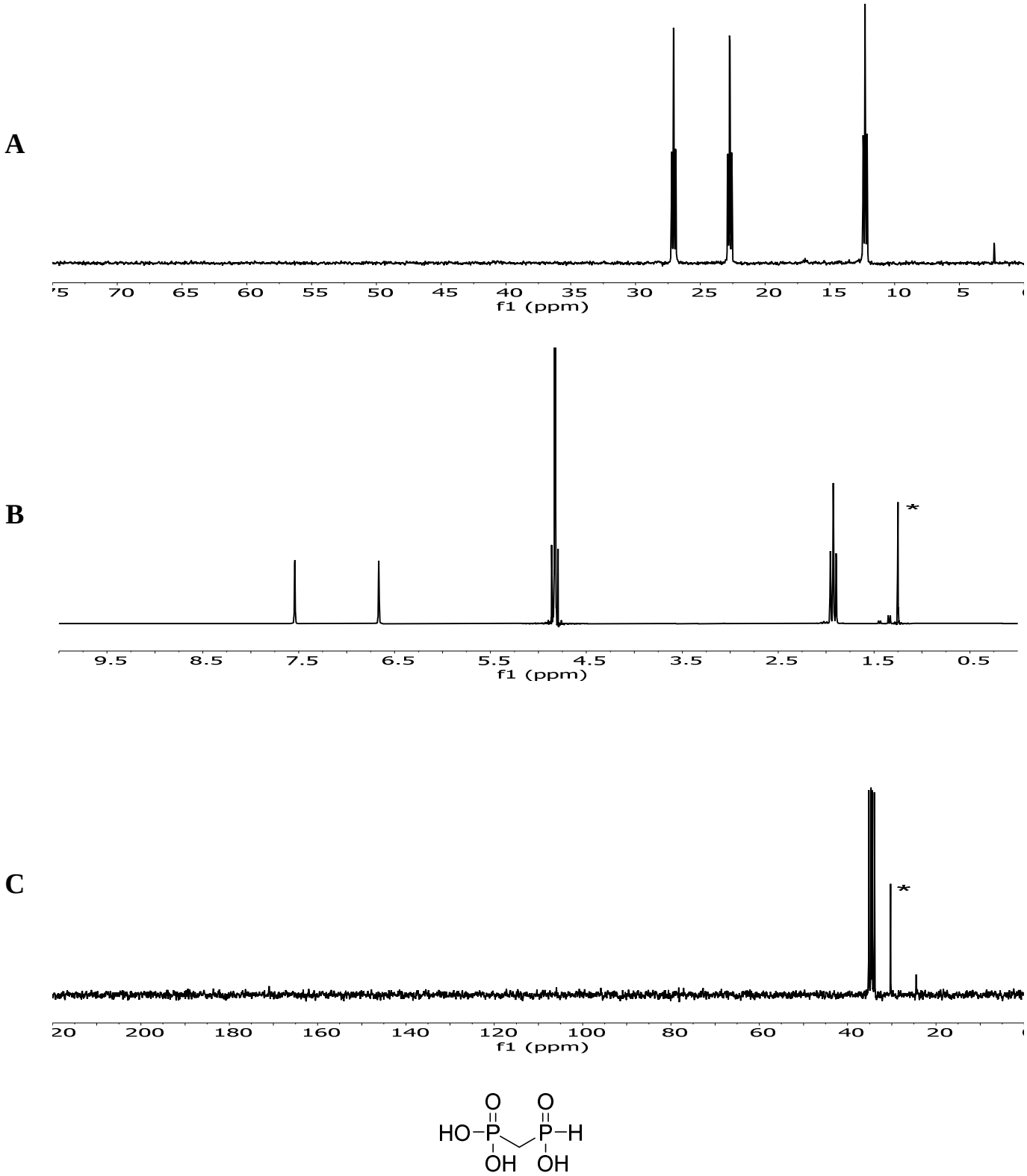

Figure S7. Characterization ^{31}P (**A**), ^{1}H (**B**) and $^{13}C\{^{1}H\}$ (**C**) NMR spectra of **1** in H_2O+CsOH (pH ~9). Signals of *t*-BuOH was labelled *.

A

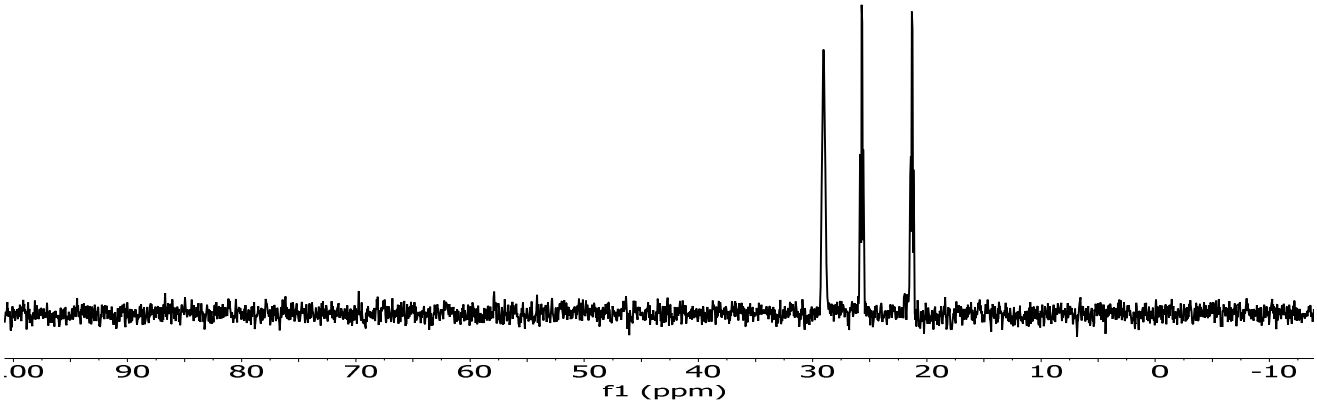

B

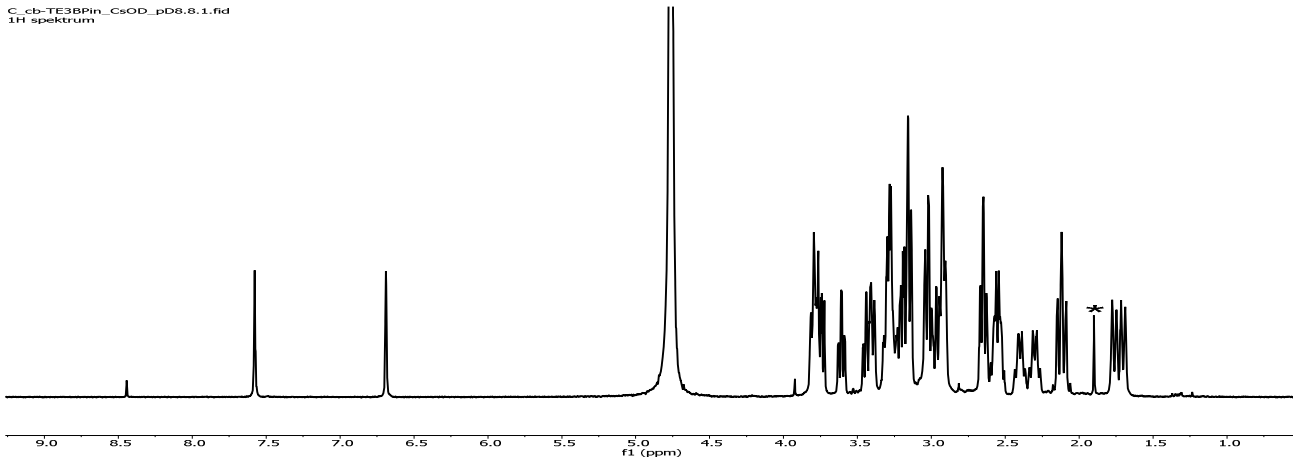

C

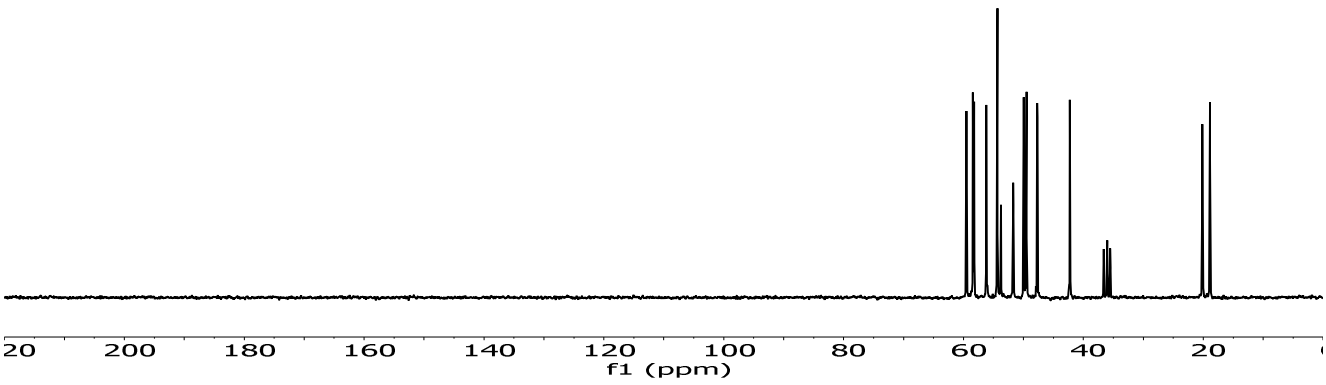

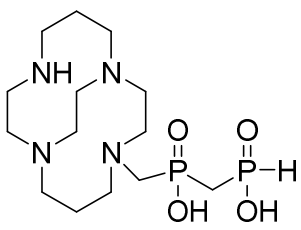

Figure S8. Characterization $^{31}P\{^{1}H\}$ (**A**), ^{1}H (**B**) and $^{13}C\{^{1}H\}$ (**C**) NMR spectra of **3** in D_2O+CsOD (pD ~10). Signals of *t*-BuOH was labelled *.

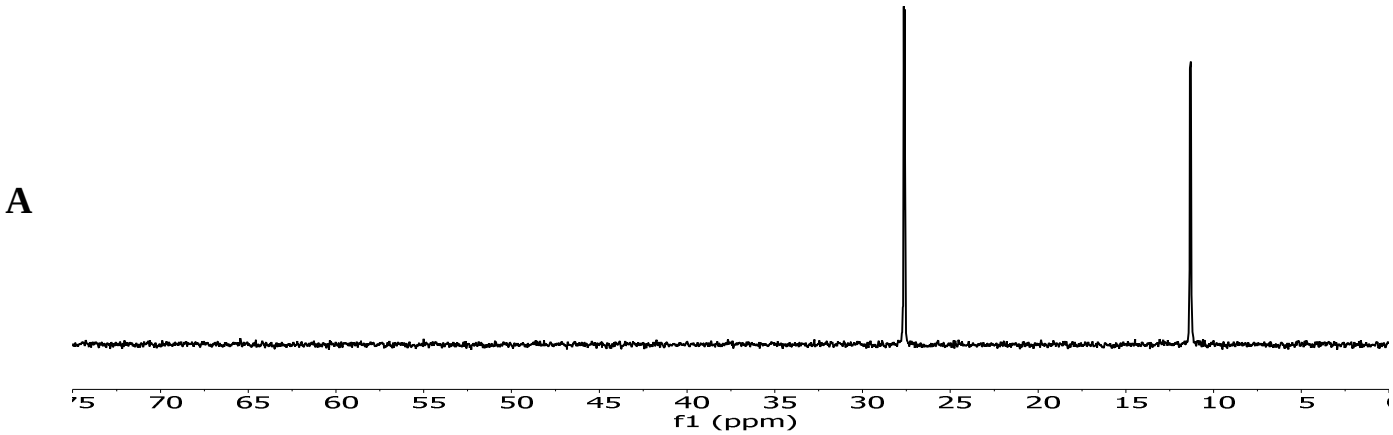

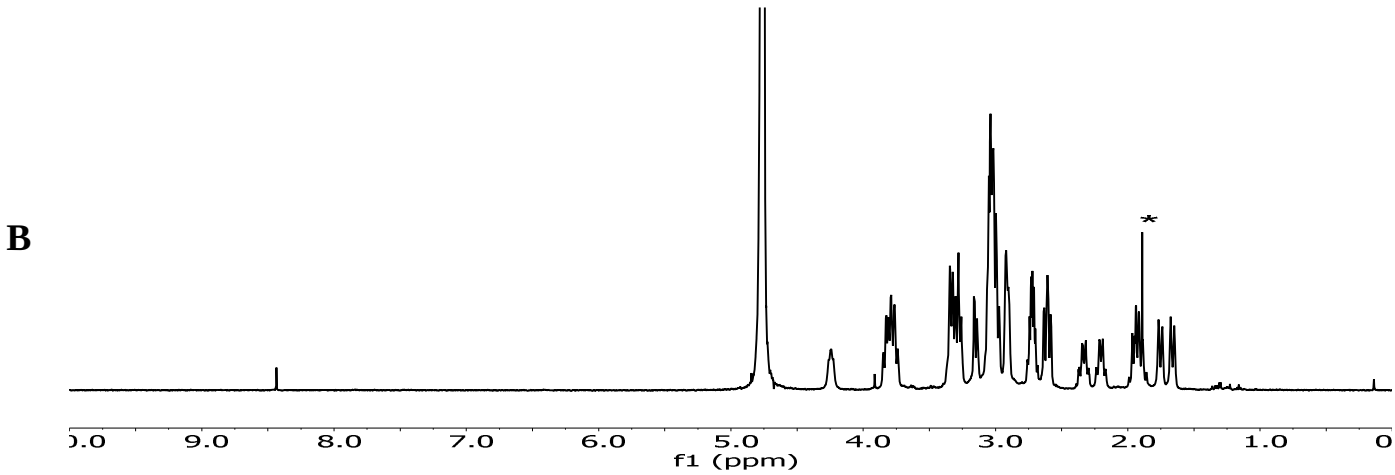

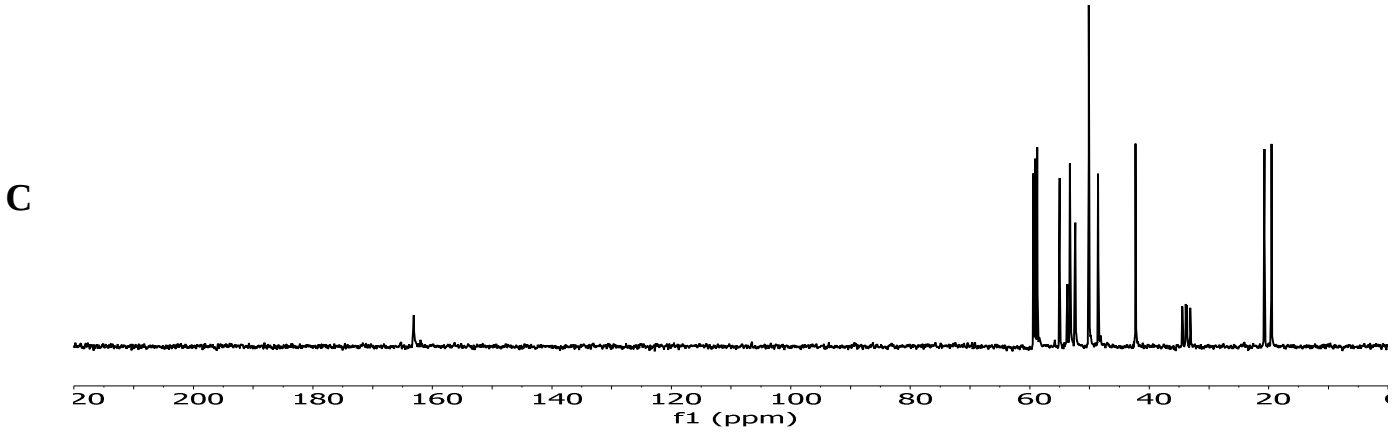

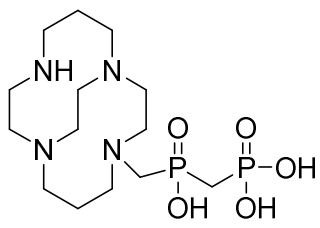

Figure S9. Characterization $^{31}P\{^{1}H\}$ (**A**), ^{1}H (**B**) and $^{13}C\{^{1}H\}$ (**C**) NMR spectra of **4** in D_2O+CsOD (pD ≥ 12). Signals of *t*-BuOH were labelled *.

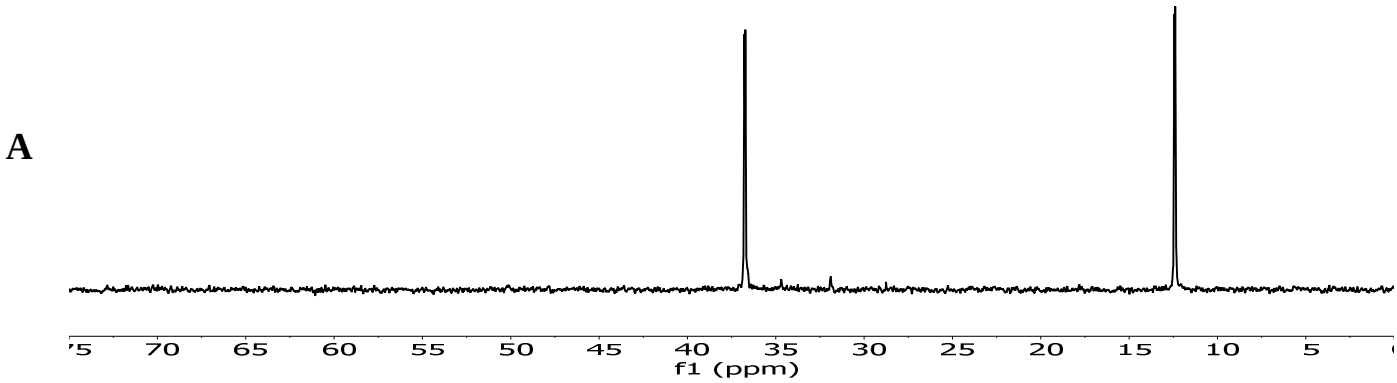

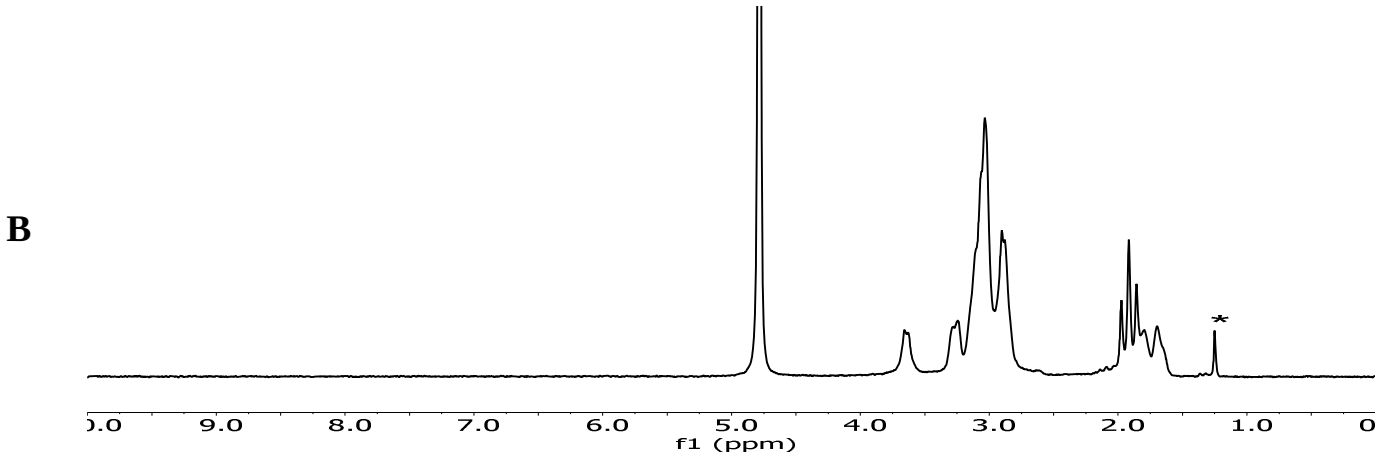

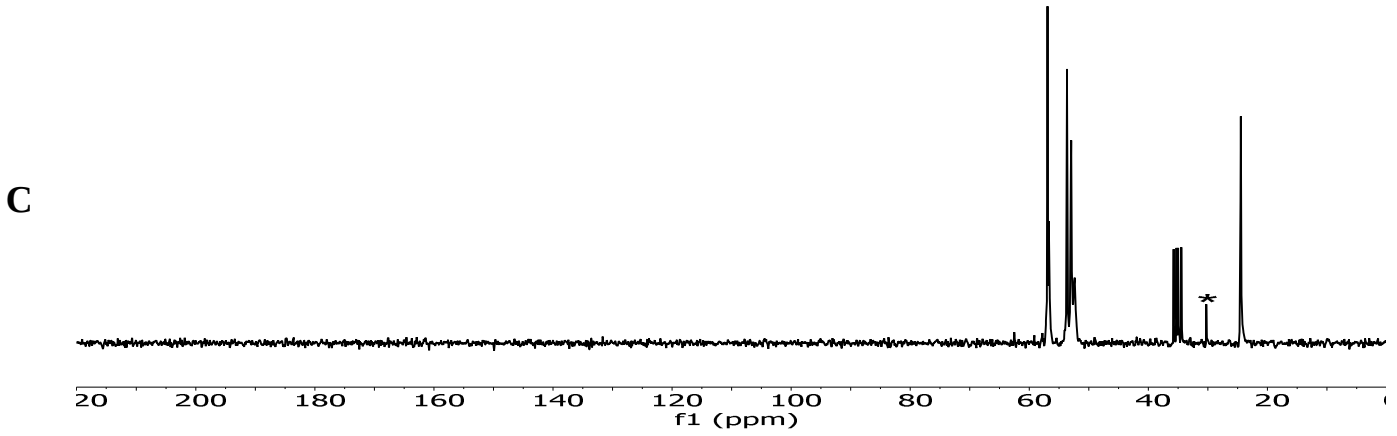

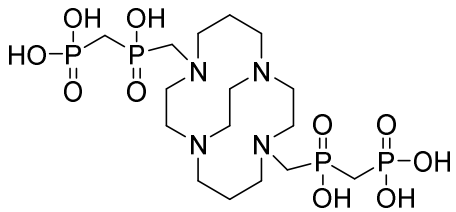

Figure S10. Characterization ^{31}P (**A**), ^{1}H (**B**) and $^{13}C\{^{1}H\}$ (**C**) NMR spectra of **5** in H_2O (pH ~1.2) with *H*-insert. Residual water signal after pre-saturation in **B** (around 4.8 ppm, labelled *) was removed for clarity reasons and signals of *t*-BuOH were labelled *.

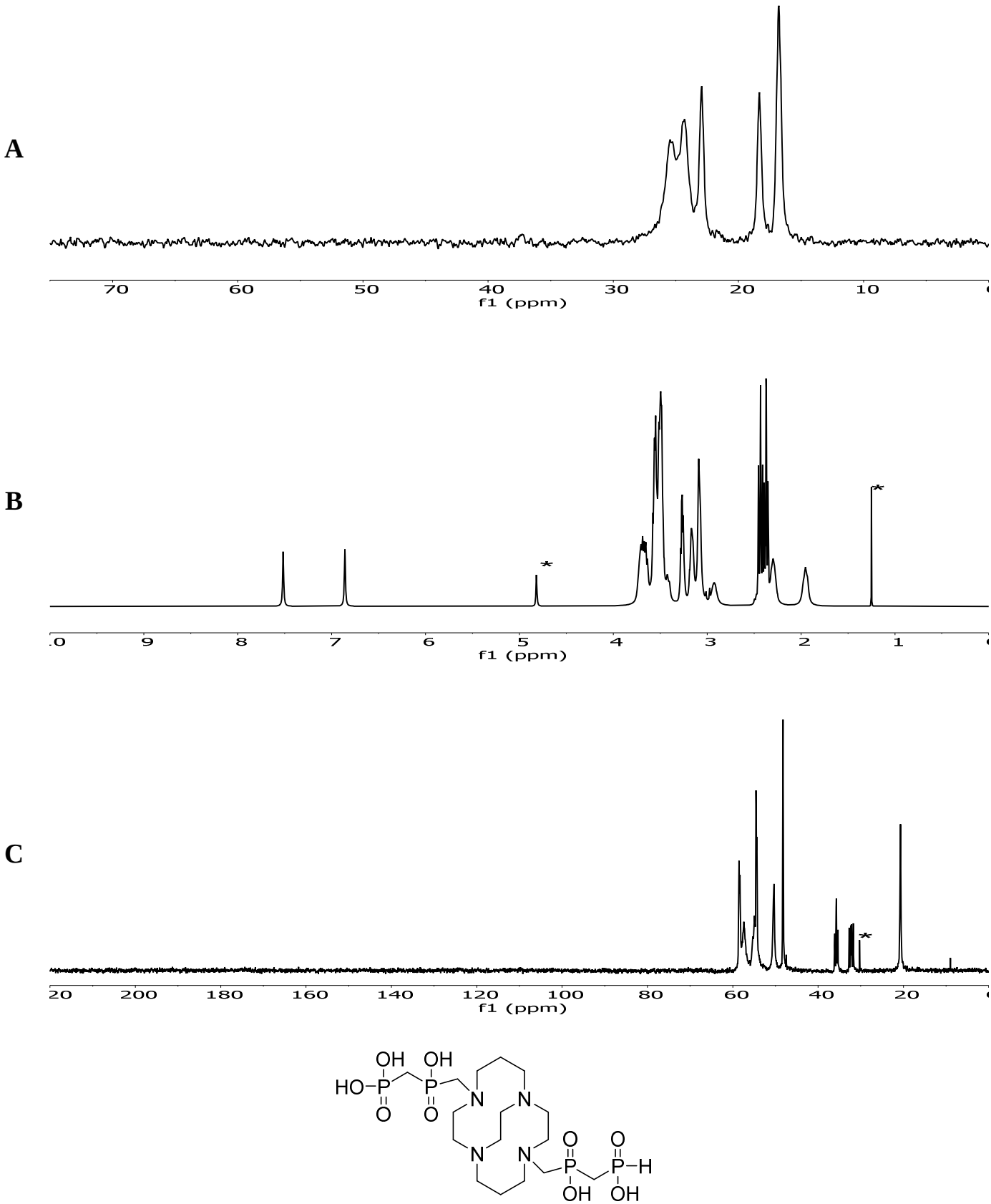

Figure S11. Characterization $^{31}P\{^{1}H\}$ (**A**), ^{1}H (**B**) and $^{13}C\{^{1}H\}$ (**C**) NMR spectra (purity >95 %) of **6** in D_2O (pD ~1.8). Residual signals of compound **7** (**A**) originating from oxidation of P–H bond and acetonitrile (**B** and **C**) were labelled *. Signals of *t*-BuOH were labelled *.

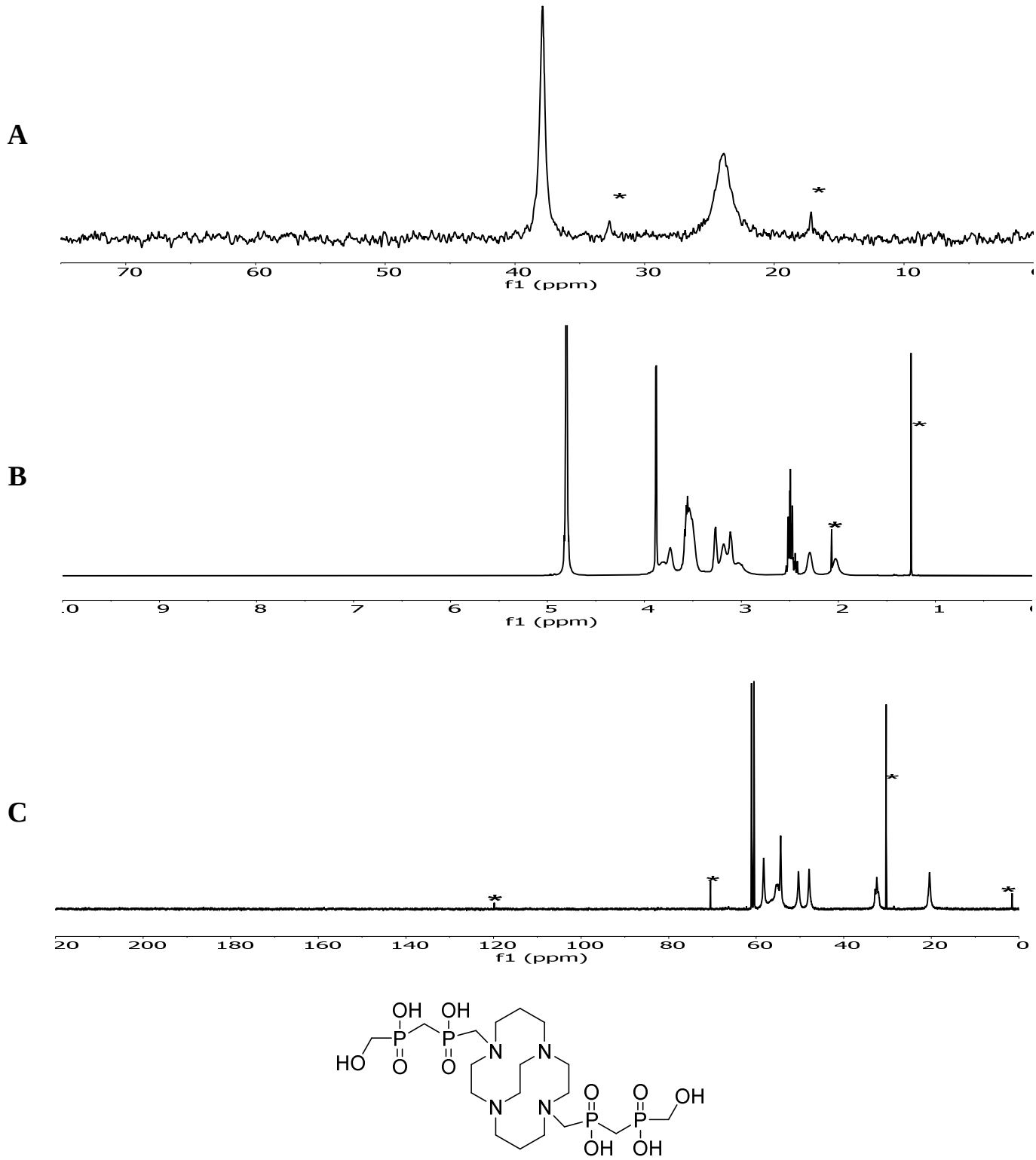

Figure S12. Characterization $^{31}P\{^{1}H\}$ (**A**), ^{1}H (**B**) and $^{13}C\{^{1}H\}$ (**C**) NMR spectra of **7** in D_2O (pD ~1.6). The residual TFA signals **C** (around 125 ppm) are labelled *. Signals of *t*-BuOH were labelled *.

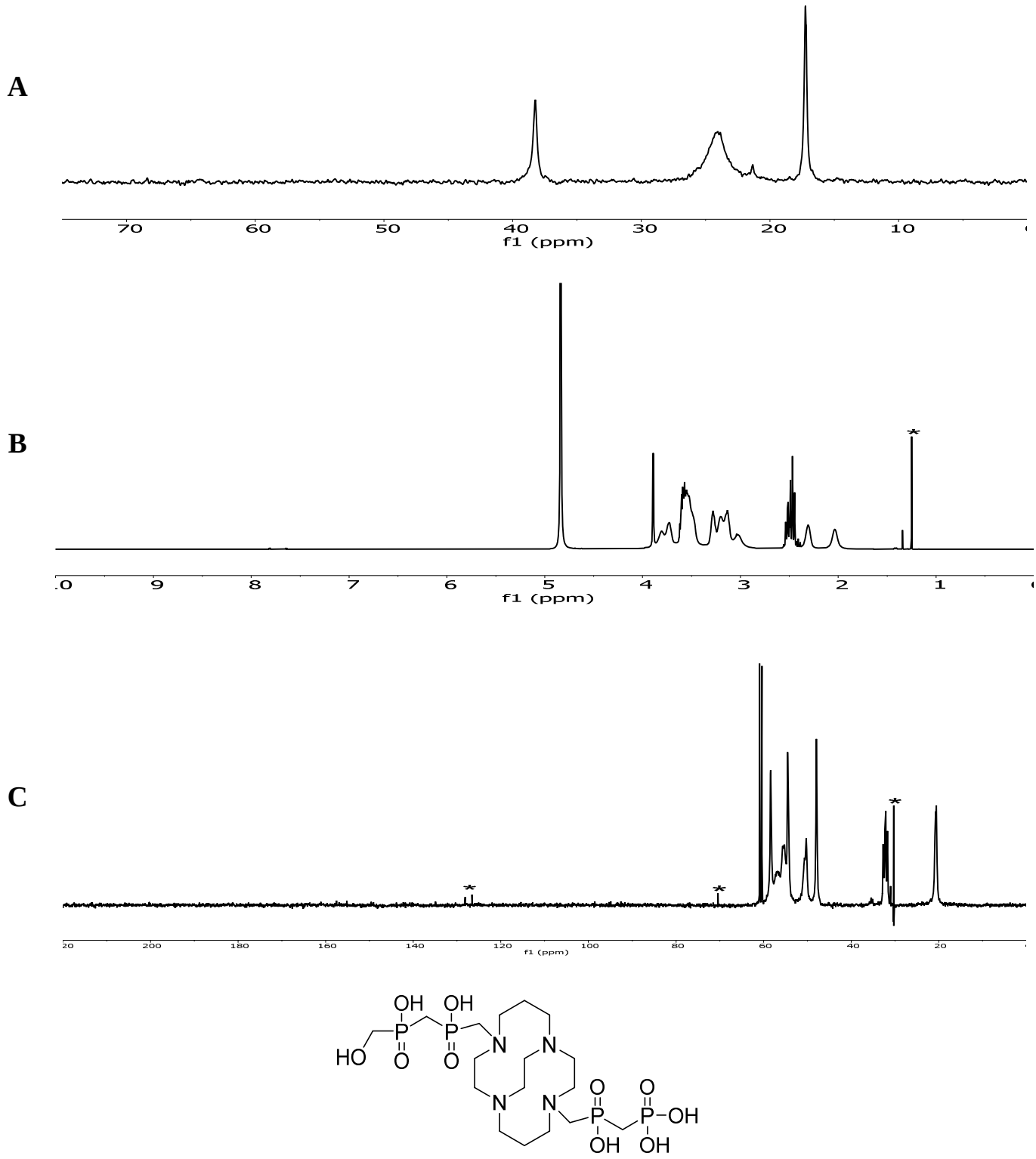

Figure S13. Characterization $^{31}P\{^{1}H\}$ (**A**), ^{1}H (**B**) and $^{13}C\{^{1}H\}$ (**C**) NMR spectra of **8** in D_2O (pD ~3).

A

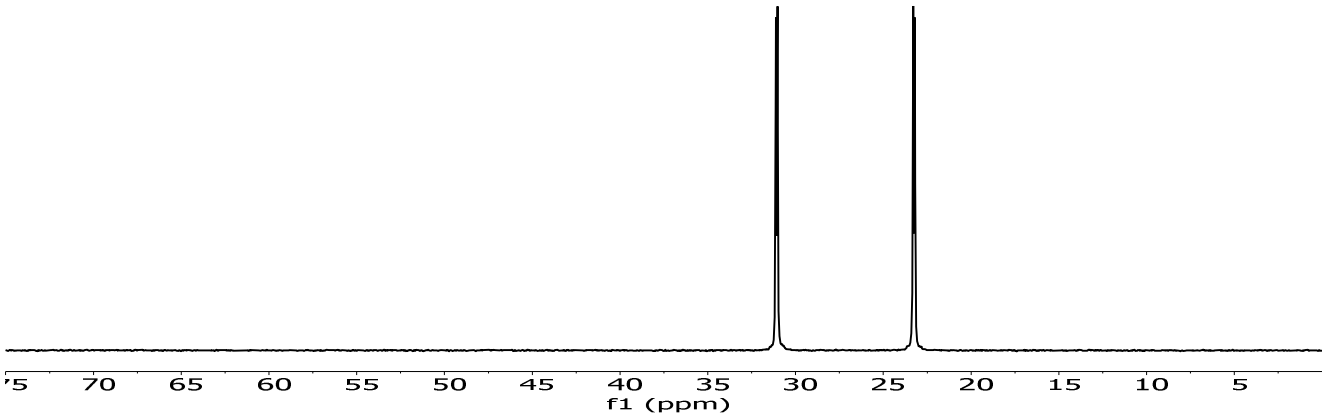

B

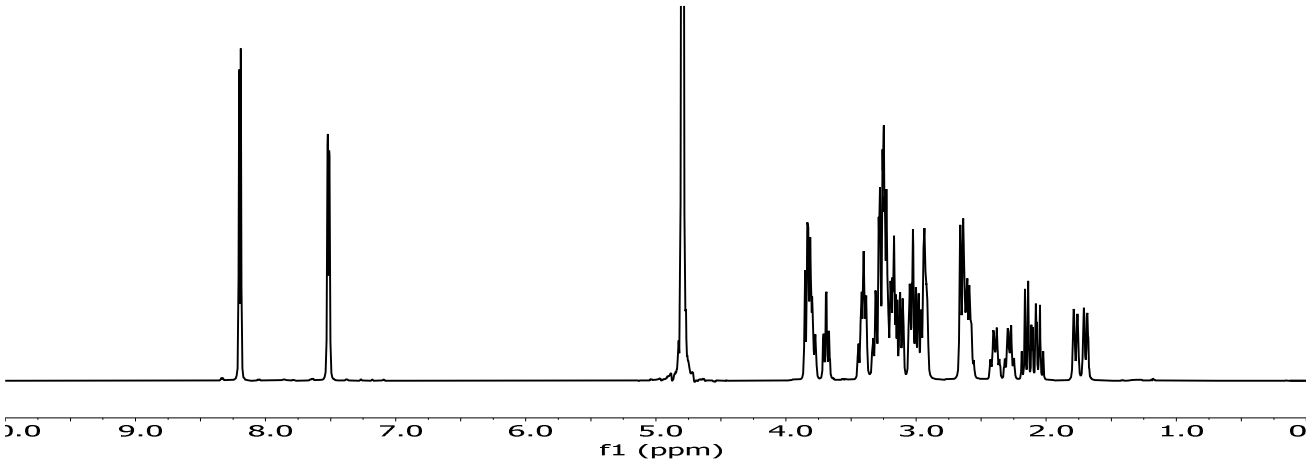

C

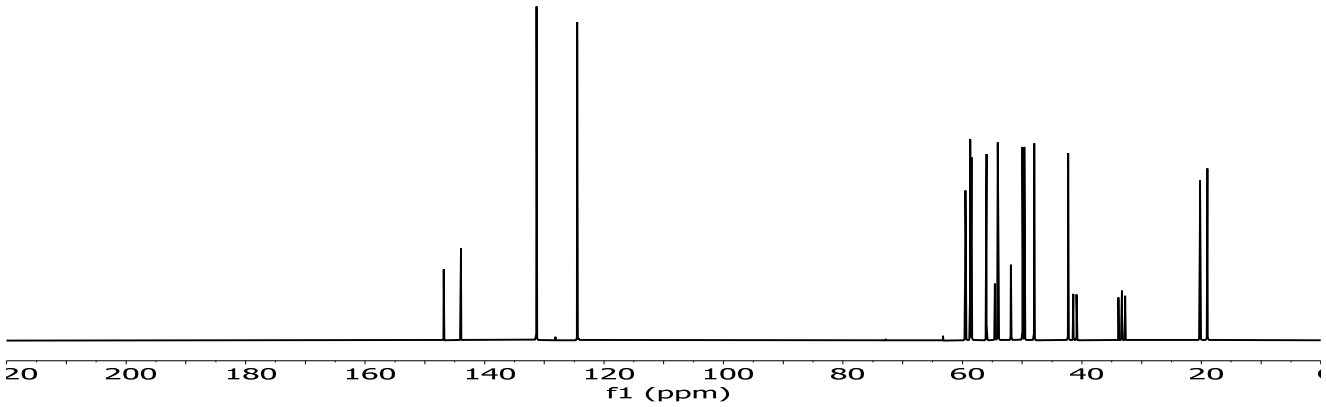

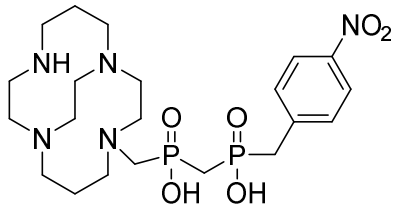

Figure S14. Characterization $^{31}P\{^{1}H\}$ (**A**), ^{1}H (**B**) and $^{13}C\{^{1}H\}$ (**C**) NMR spectra of **9** in D_2O+CsOD (pD ~11). The residual TFA and acetonitrile signals in **B** and **C** are labelled *. Signals of *t*-BuOH were labelled *.

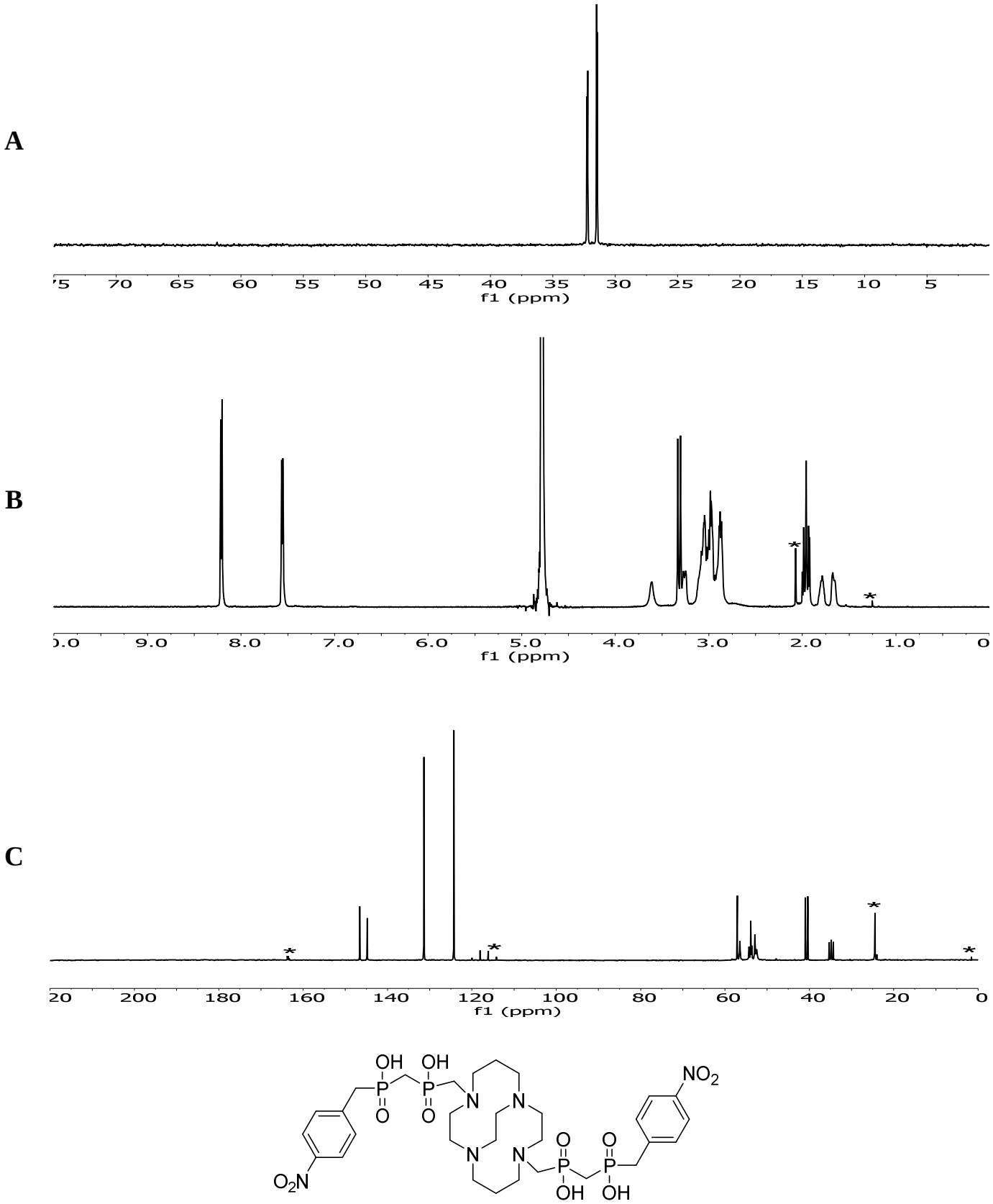

Figure S15. Characterization $^{31}P\{^{1}H\}$ (**A**), ^{1}H (**B**) and $^{13}C\{^{1}H\}$ (**C**) NMR spectra of **10** (purity ≥95%) in D_2O (pD ≤ 1). Signals of *t*-BuOH were labelled *.

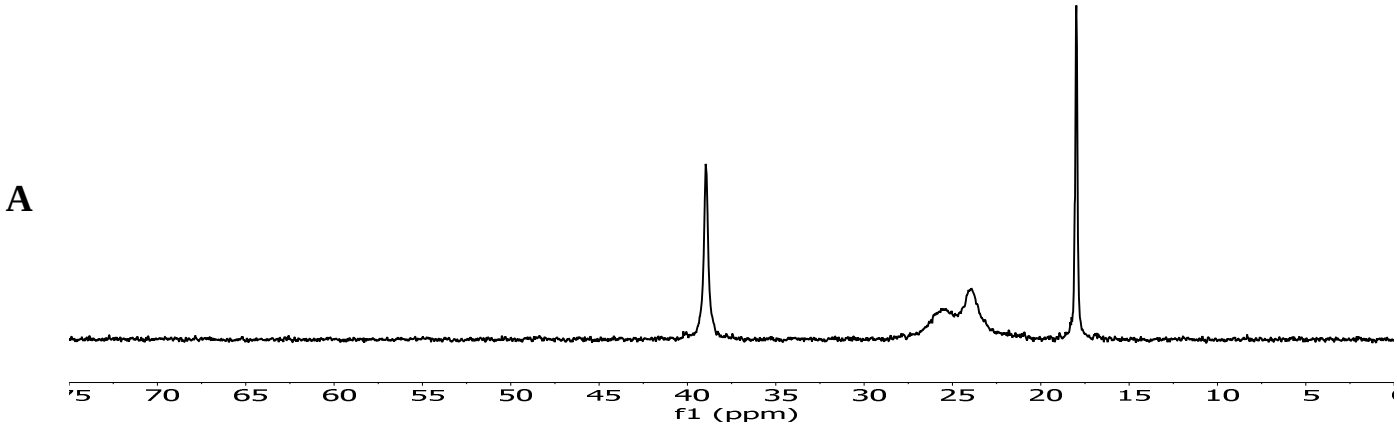

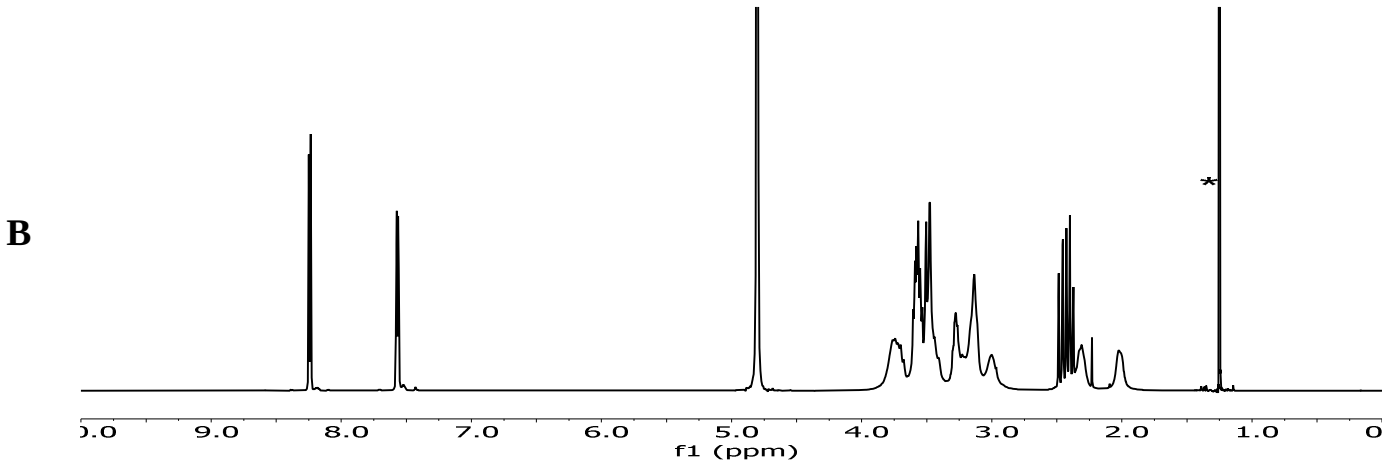

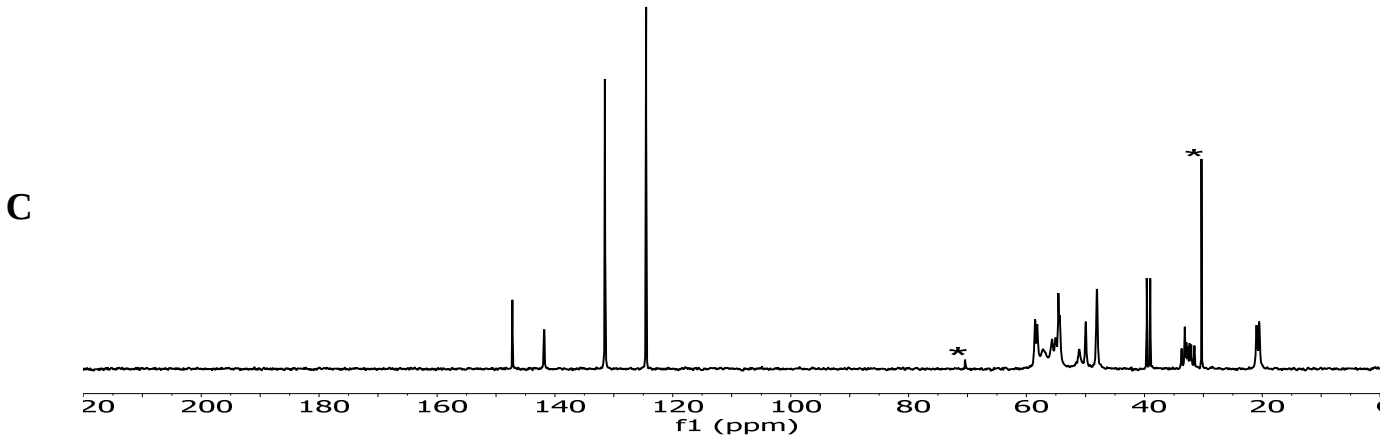

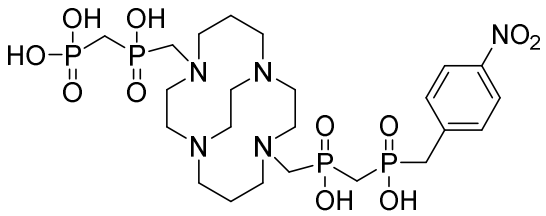

Figure S16. Characterization $^{31}P\{^{1}H\}$ (**A**), ^{1}H (**B**) and $^{13}C\{^{1}H\}$ (**C**) NMR spectra of **11** (purity >90 %) in H_2O (pH ~1.8). Residual signals of TFA in **C** are labelled *. Signals of *t*-BuOH were labelled *.

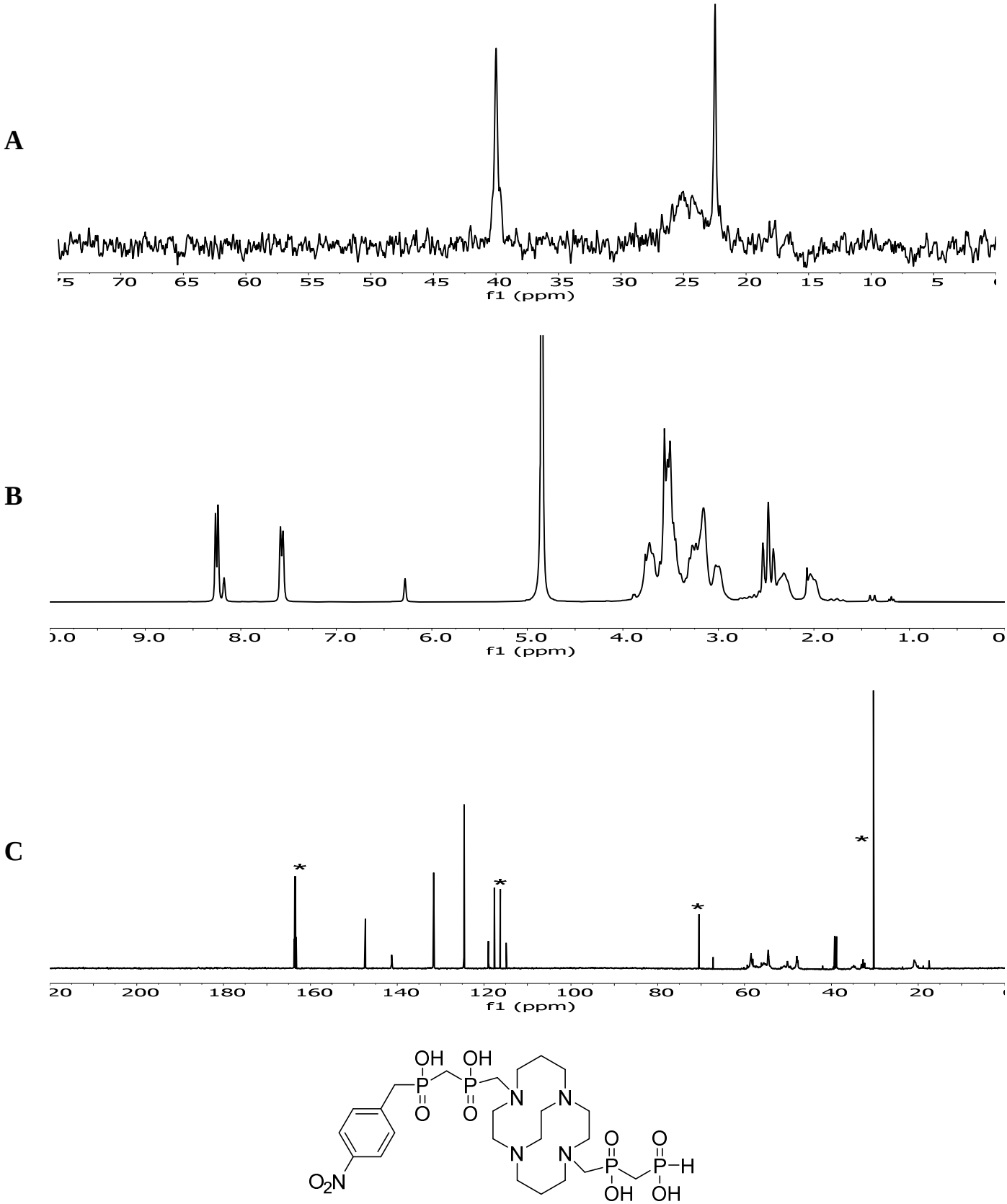

Figure S17. Characterization $^{31}P\{^{1}H\}$ (**A**), ^{1}H (**B**) and $^{13}C\{^{1}H\}$ (**C**) NMR spectra (purity >95 %) of **12** in D_2O (pD ~1.7). Residual signals of compound **10** in **A** and TFA in **C** are labelled *. Signals of *t*-BuOH were labelled *.

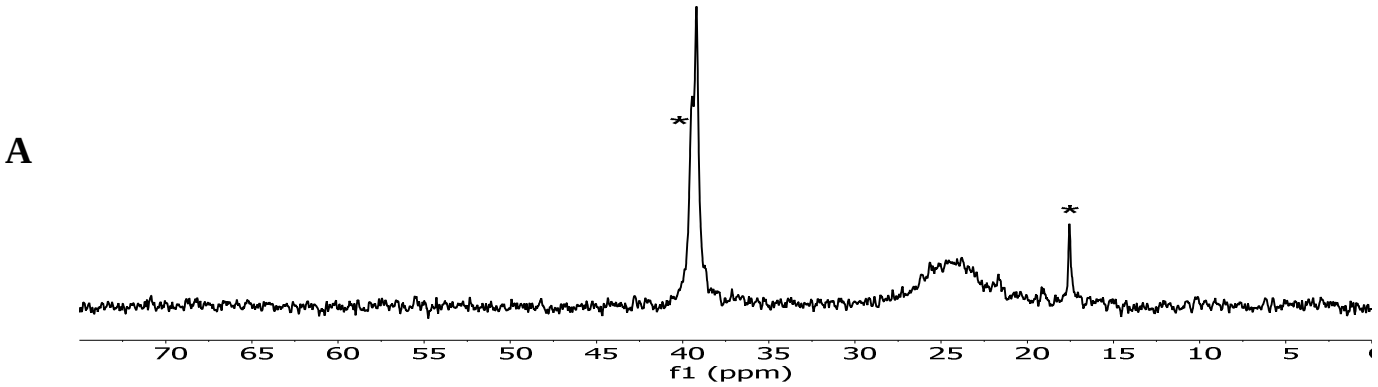

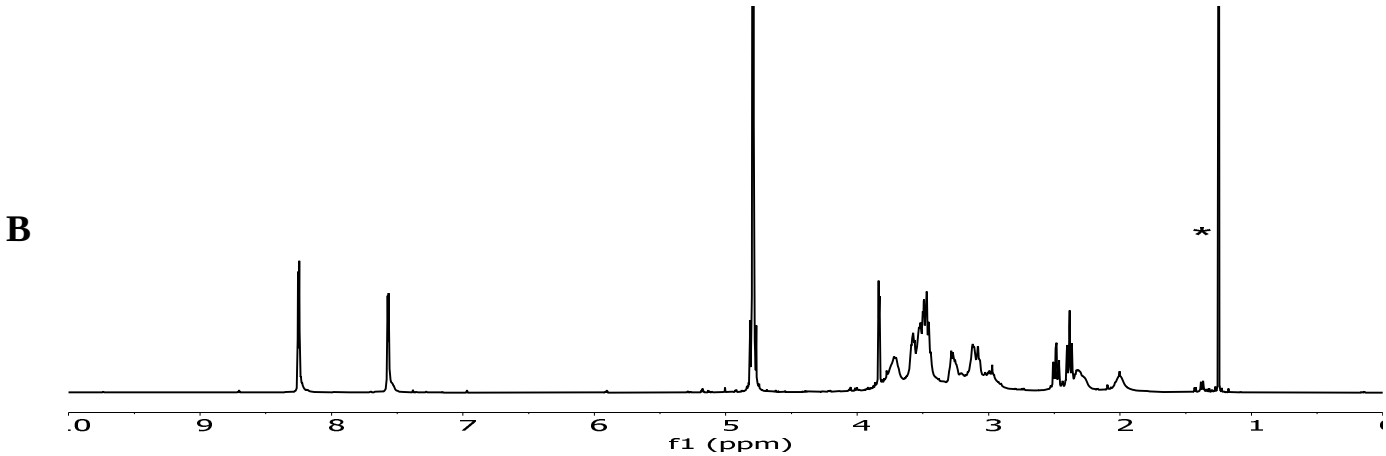

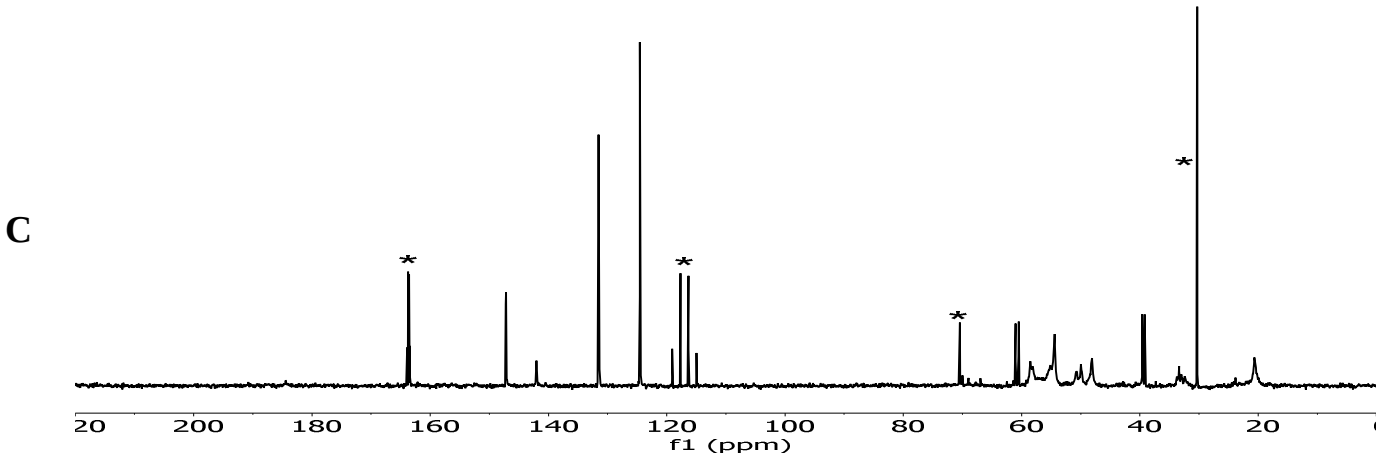

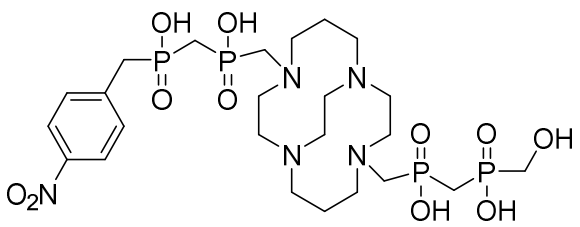

Figure S18. Characterization $^{31}P\{^{1}H\}$ (**A**) and ^{1}H (**B**) NMR spectra of **13a** in D_2O (pD ~1.6). Signals of *t*-BuOH were labelled *.

A

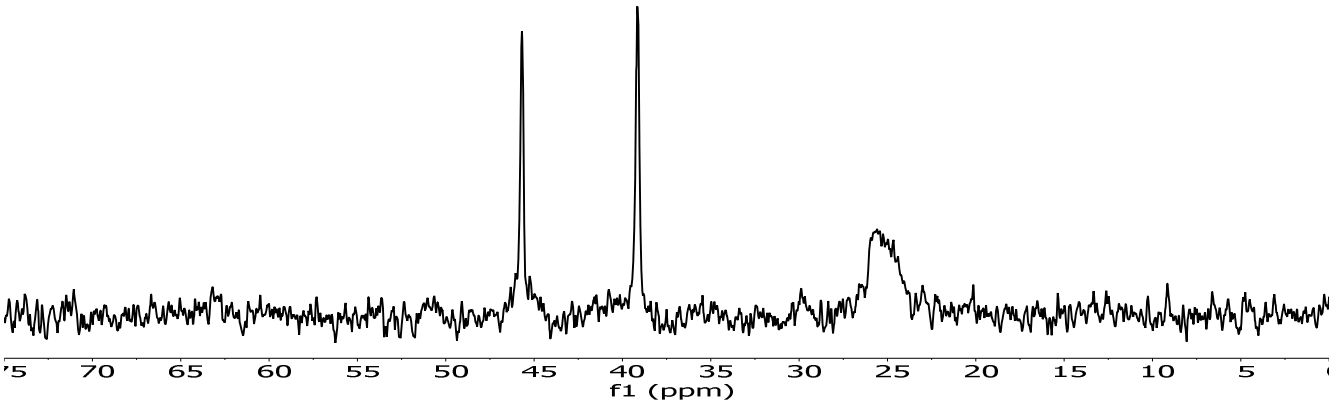

B

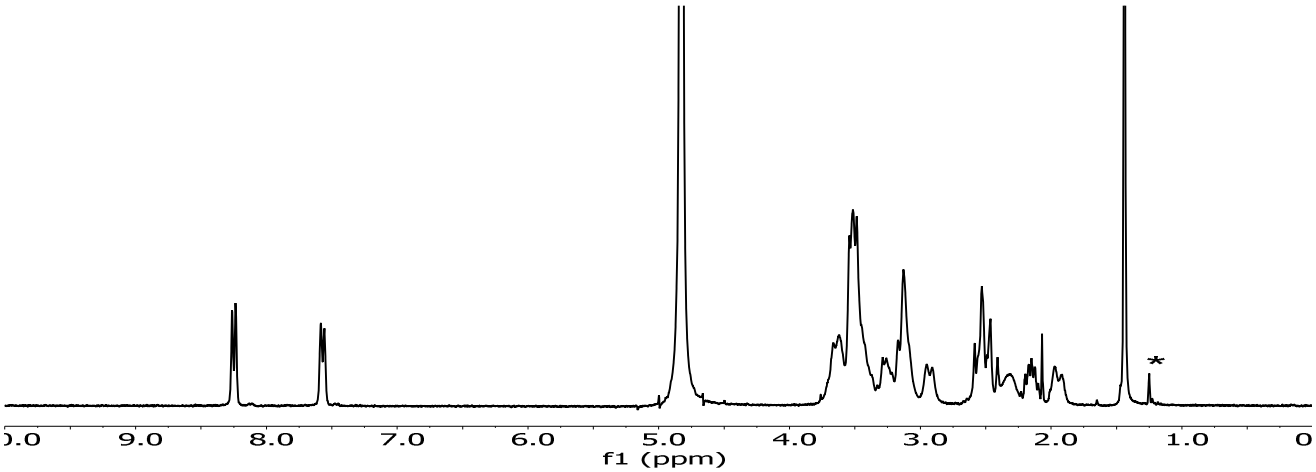

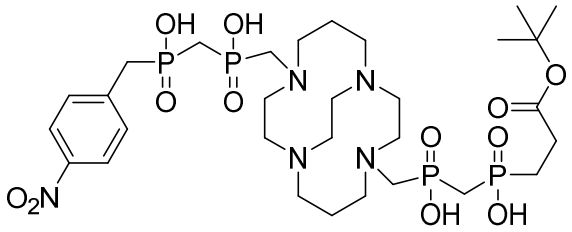

Figure S19. Characterization $^{31}P\{^{1}H\}$ (**A**), ^{1}H (**B**) and $^{13}C\{^{1}H\}$ (**C**) NMR spectra of **13** in D_2O (pD ~1.1). Residual signals of TFA in **C** are labelled *. Signals of *t*-BuOH were labelled *.

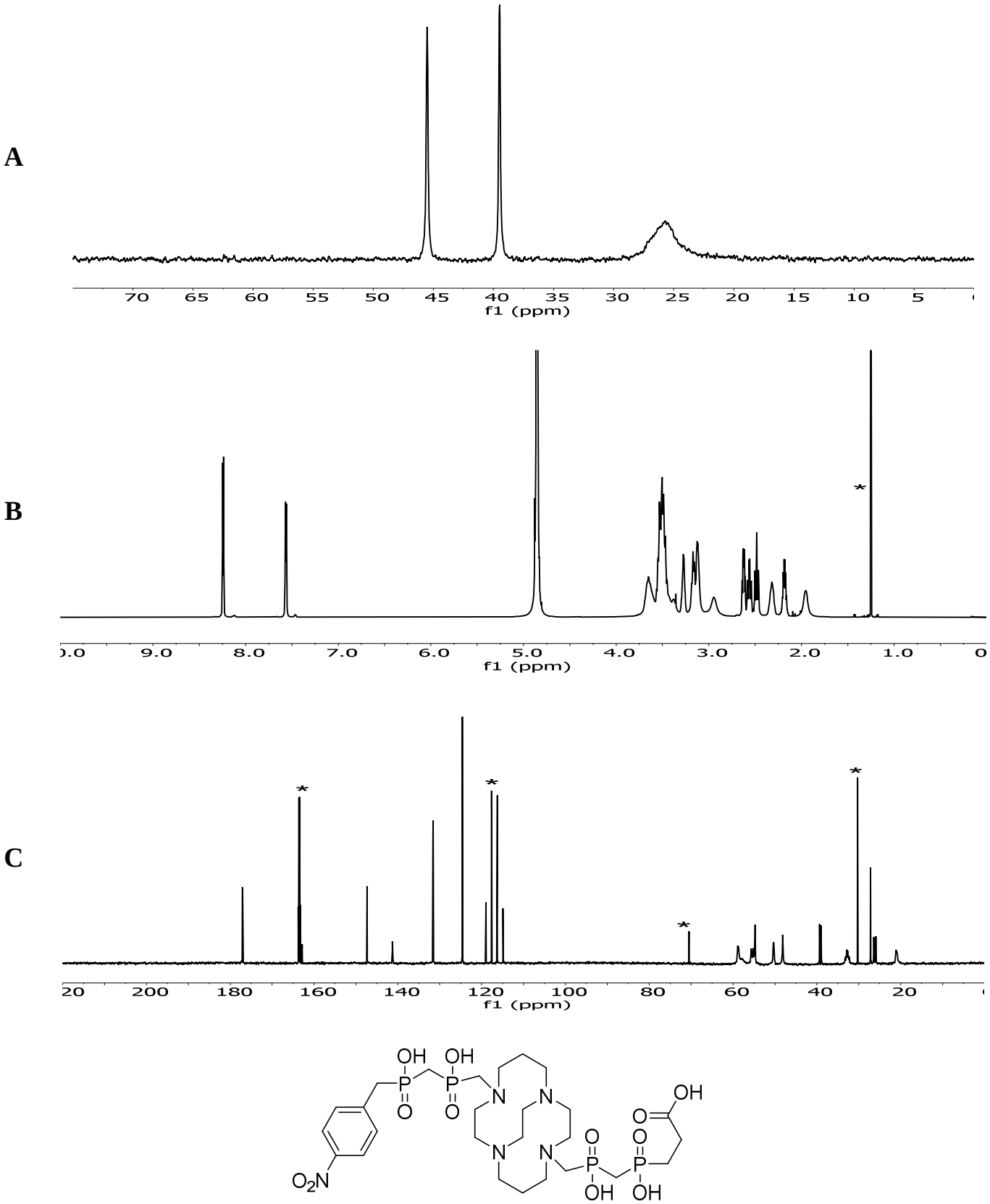

Figure S20. Characterization $^{31}P\{^{1}H\}$ (**A**), ^{1}H (**B**) and $^{13}C\{^{1}H\}$ (**C**) NMR spectra of **14** in D_2O (pD ~1.5). Residual signals of TFA in **C** are labelled *. Signals of *t*-BuOH were labelled *.

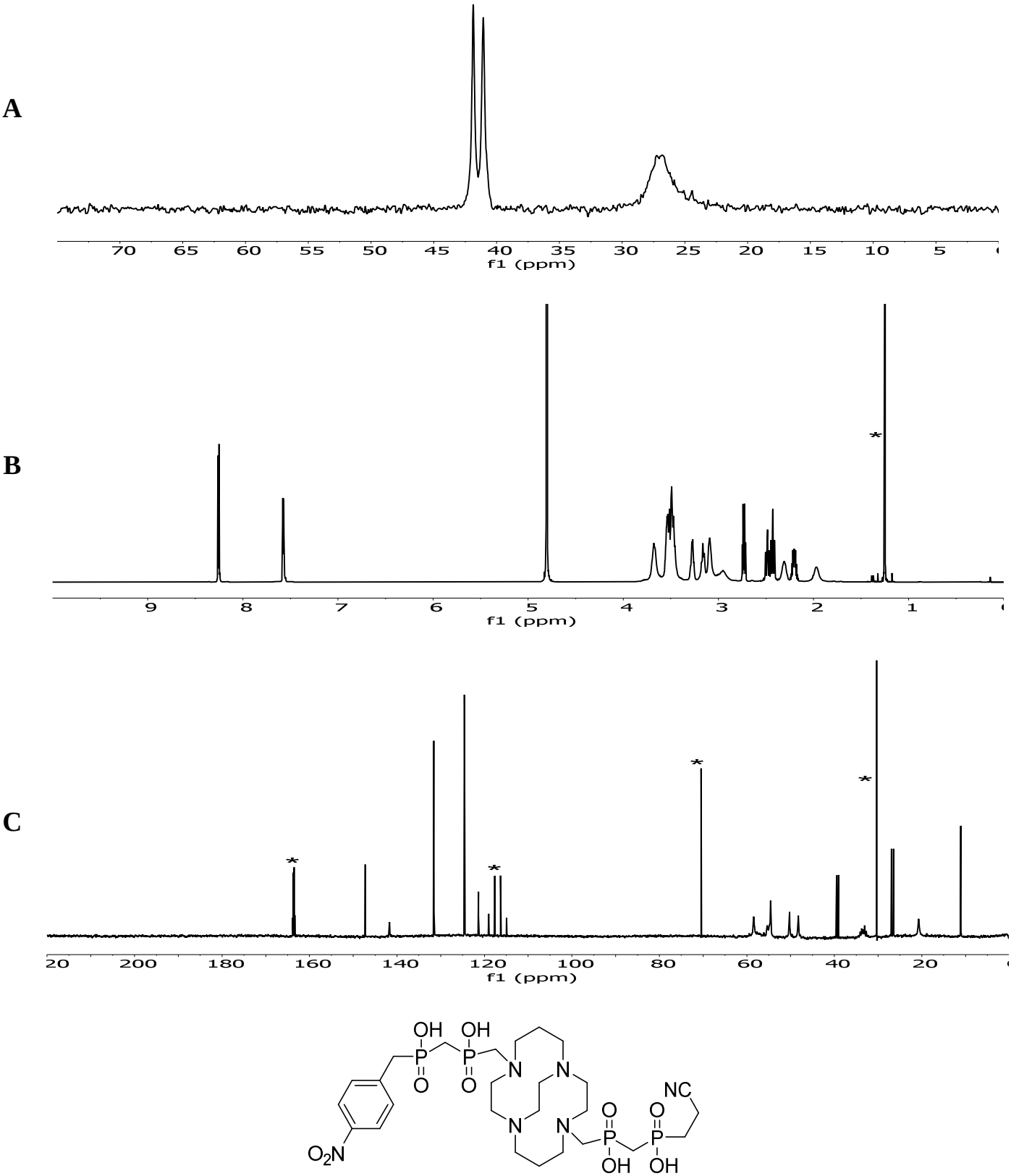

Figure S21. Characterization $^{31}P\{^{1}H\}$ (**A**), ^{1}H (**B**) and $^{13}C\{^{1}H\}$ (**C**) NMR spectra of racemic **15a** in D_2O (pD ~1.8). Residual signals of TFA in **C** are labelled *. Signals of *t*-BuOH were labelled *.

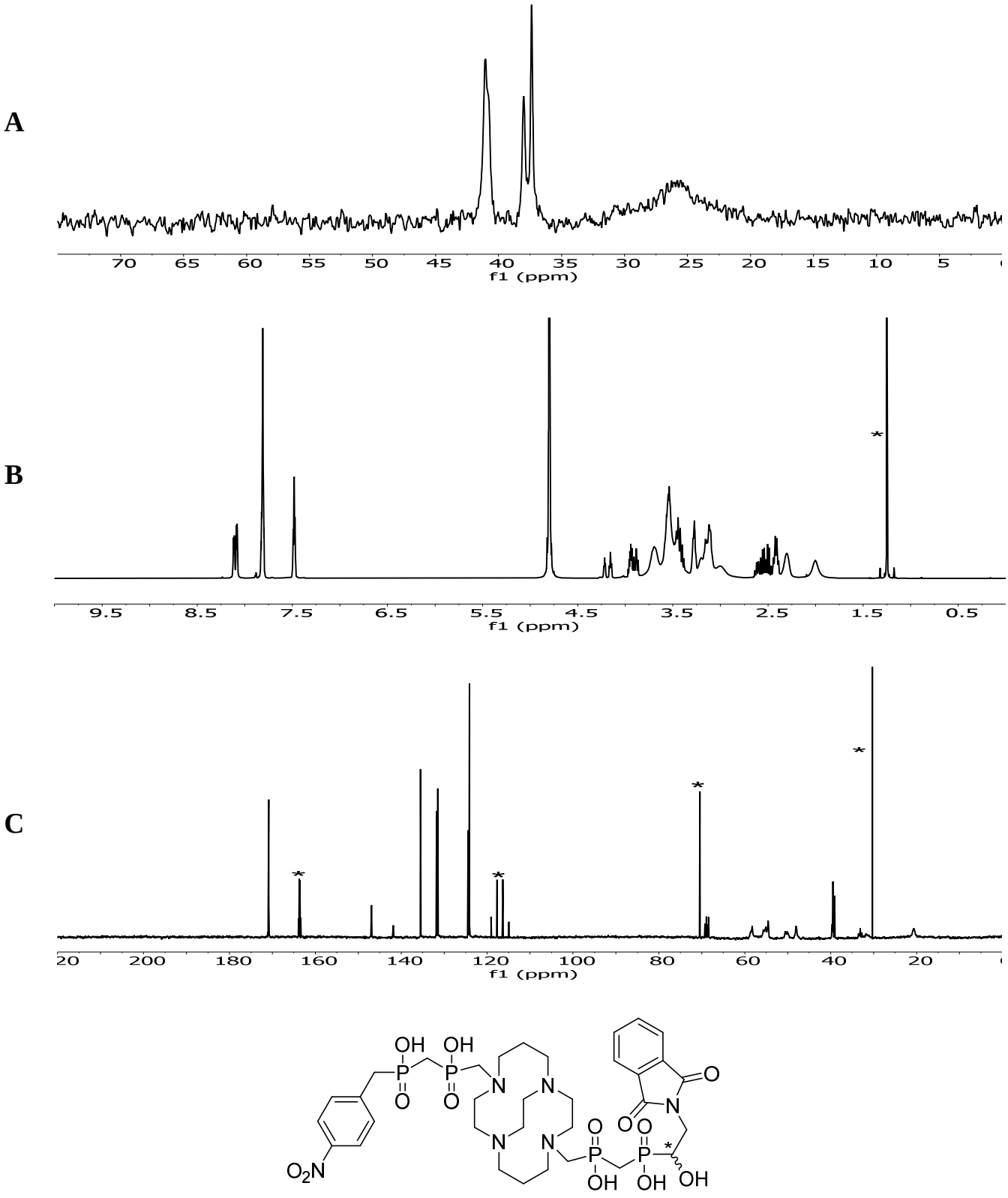

The multiple peaks seen in the NMR spectra are probably connected with a “locked” macrocycle conformation and presence of both enantiomers.

Figure S22. Characterization $^{31}P\{^{1}H\}$ (**A**), ^{1}H (**B**) and $^{13}C\{^{1}H\}$ (**C**) NMR spectra of **15** in D_2O (pD ~2.3). Residual signals of TFA in **C** are labelled *. Signals of *t*-BuOH were labelled *.

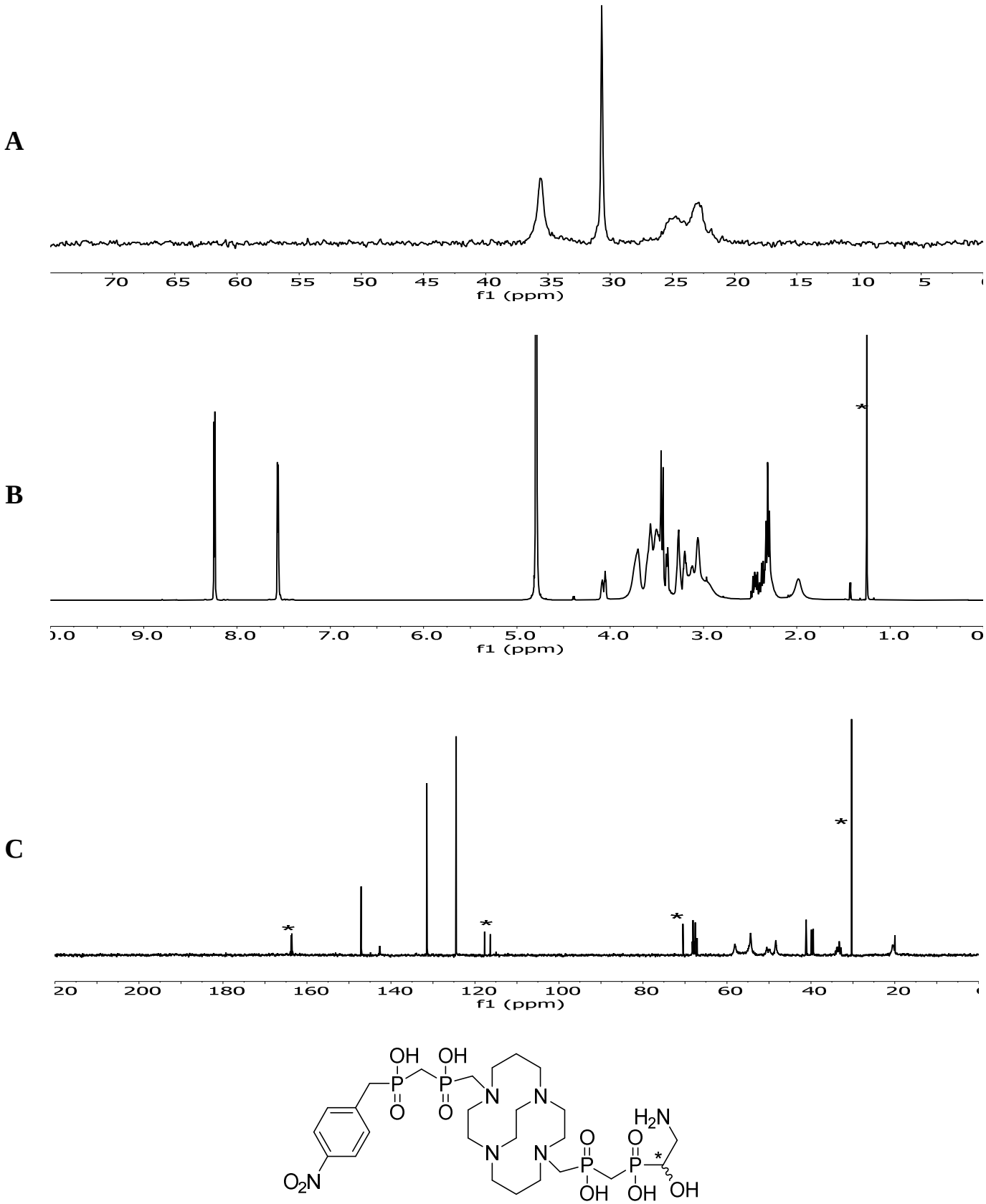

Figure S23. Characterization $^{31}P\{^{1}H\}$ (**A**), ^{1}H (**B**) and $^{13}C\{^{1}H\}$ (**C**) NMR spectra of **16** in D_2O (pD ~3).

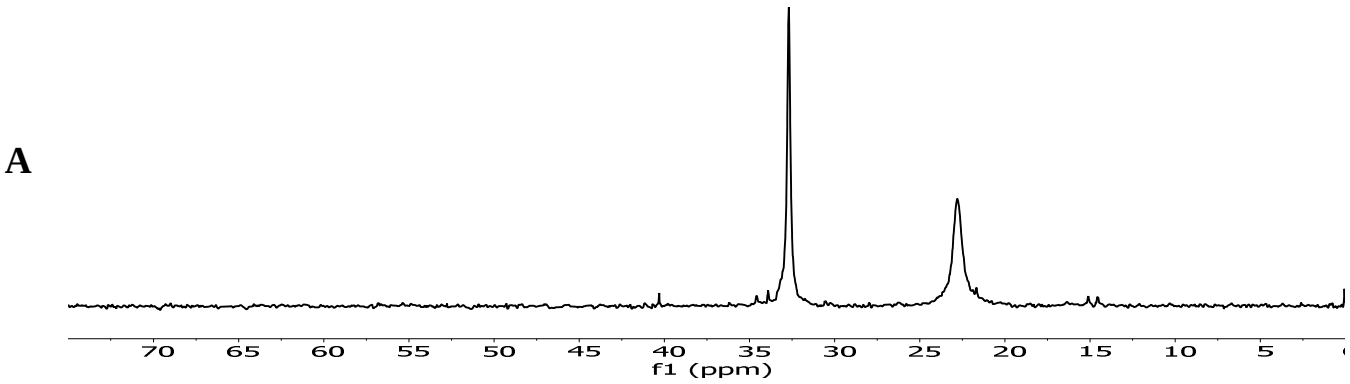

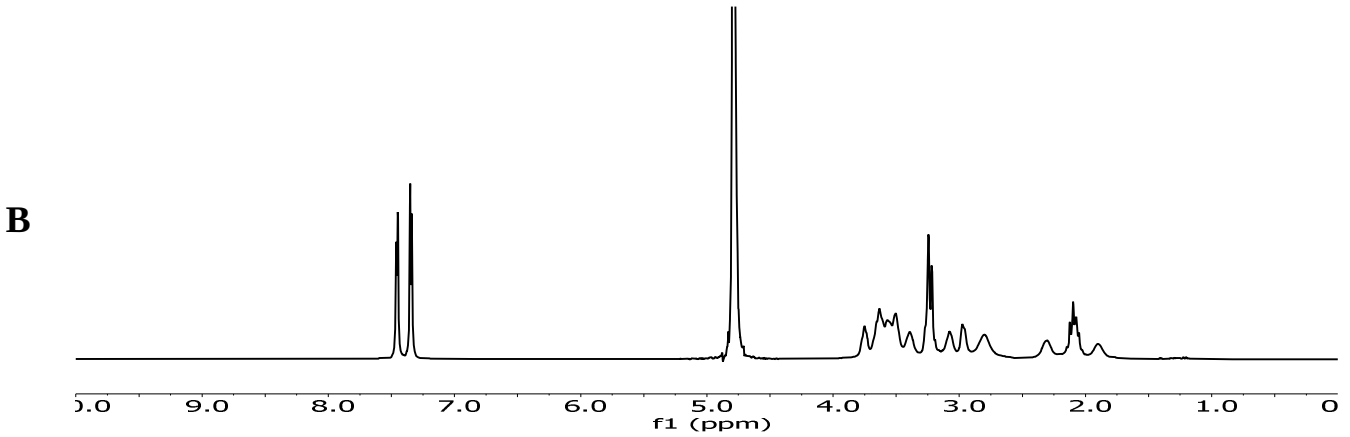

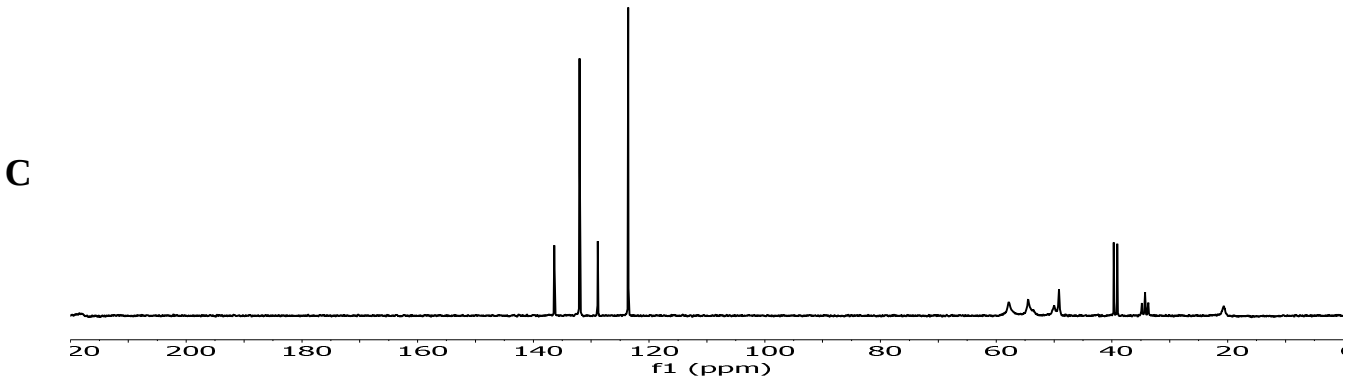

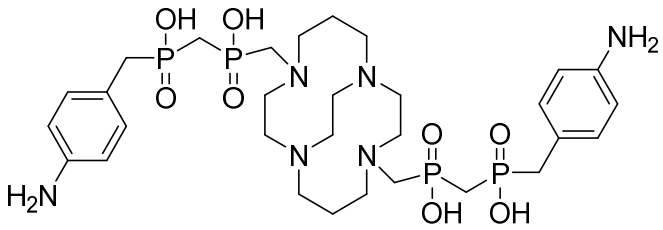

Figure S24. Characterization $^{31}P\{^{1}H\}$ (**A**), ^{1}H (**B**) and $^{13}C\{^{1}H\}$ (**C**) NMR spectra of **17** in D_2O (pD ~2). Residual water signal after pre-saturation in **B** (around 4.8 ppm, labelled *) was removed for clarity reasons.

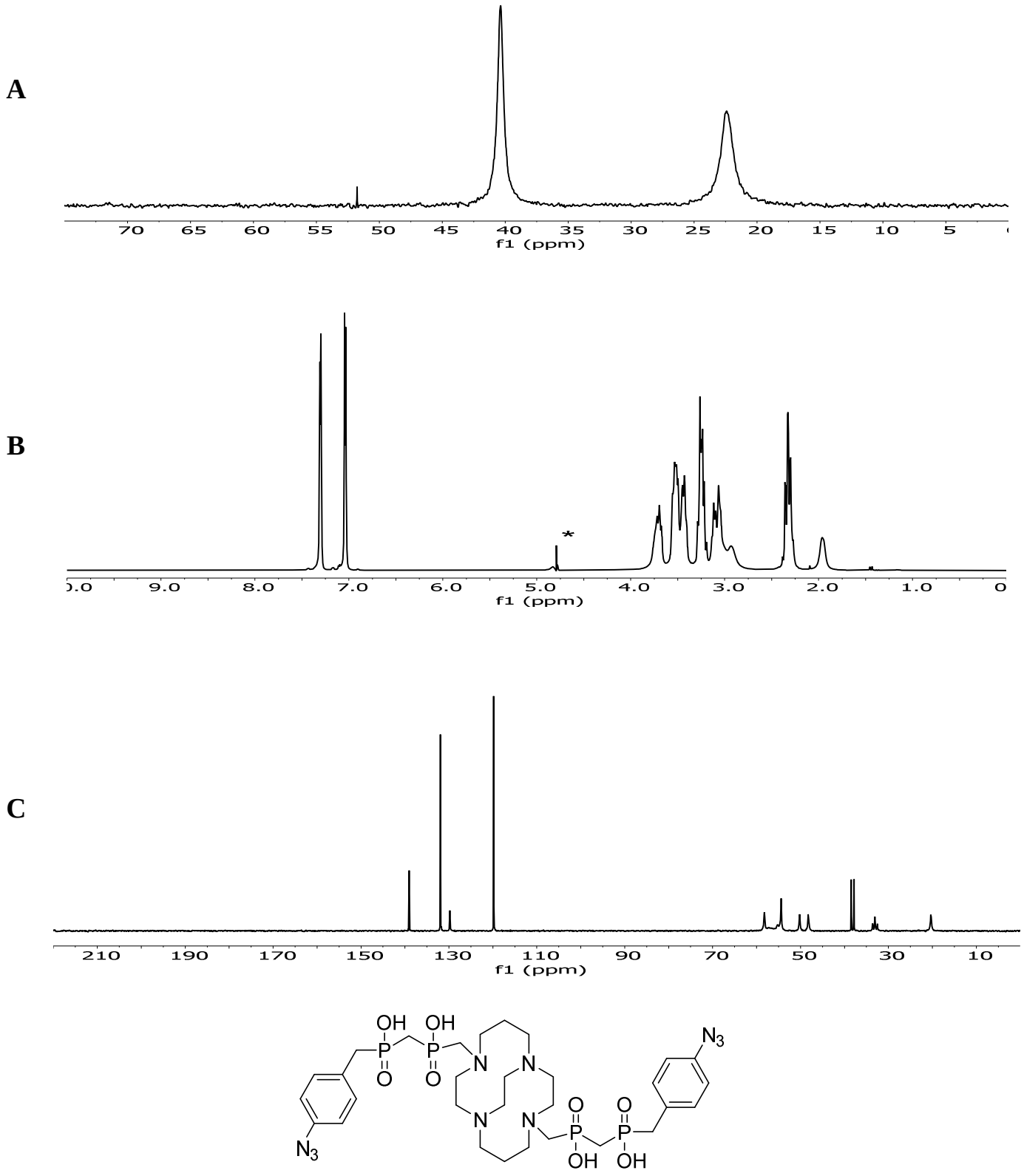

Figure S25 Characterization $^{31}P\{^{1}H\}$ (**A**), ^{1}H (**B**) and $^{13}C\{^{1}H\}$ (**C**) NMR spectra of **18** in D_2O + CsOD (pD ~2). Residual signals of TFA in **C** are labelled *.

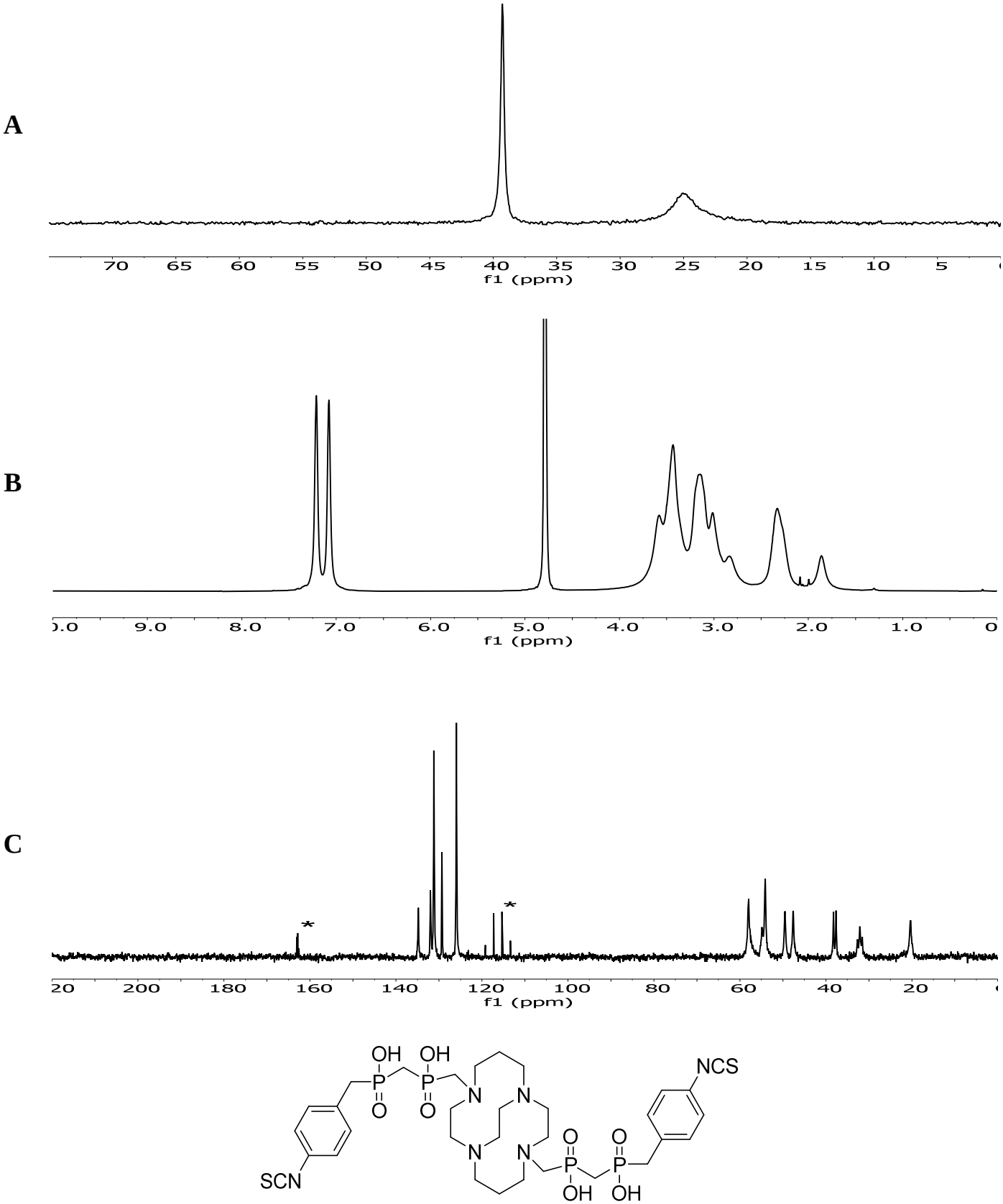

Figure S26. Characterization $^{31}P\{^{1}H\}$ (**A**), ^{1}H (**B**) and $^{13}C\{^{1}H\}$ (**C**) NMR spectra of **19** in D_2O (pD ~2). Residual water signal after pre-saturation in **B** (around 4.8 ppm, labelled *) was removed for clarity reasons. Signals of EtOH were labelled *.

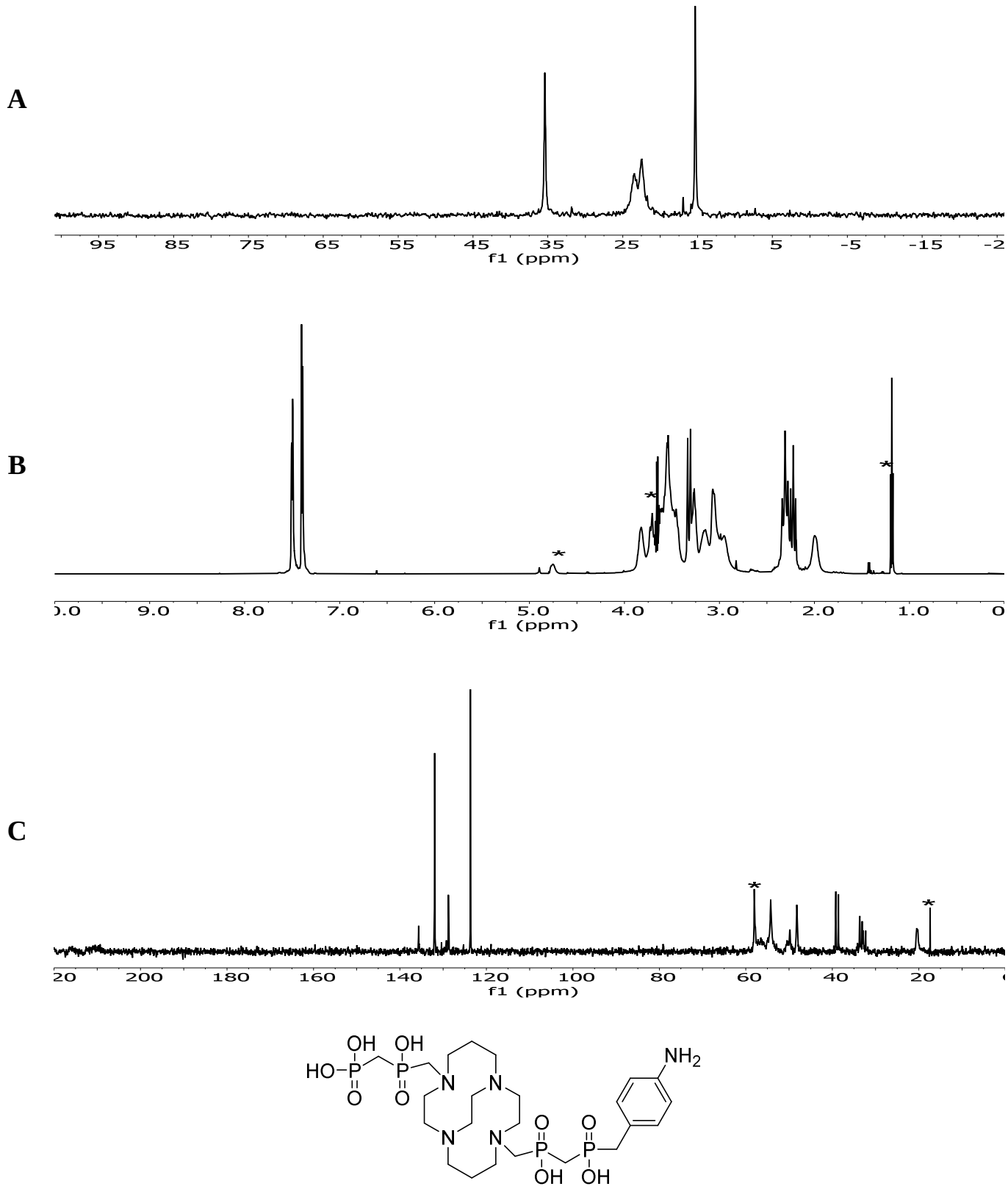

Figure S27. Characterization $^{31}P\{^{1}H\}$ (**A**), ^{1}H (**B**) and $^{13}C\{^{1}H\}$ (**C**) NMR spectra of **20** in D_2O (pD ~3). Residual water signal after pre-saturation in **B** (around 4.8 ppm, labelled *) was removed for clarity reasons.

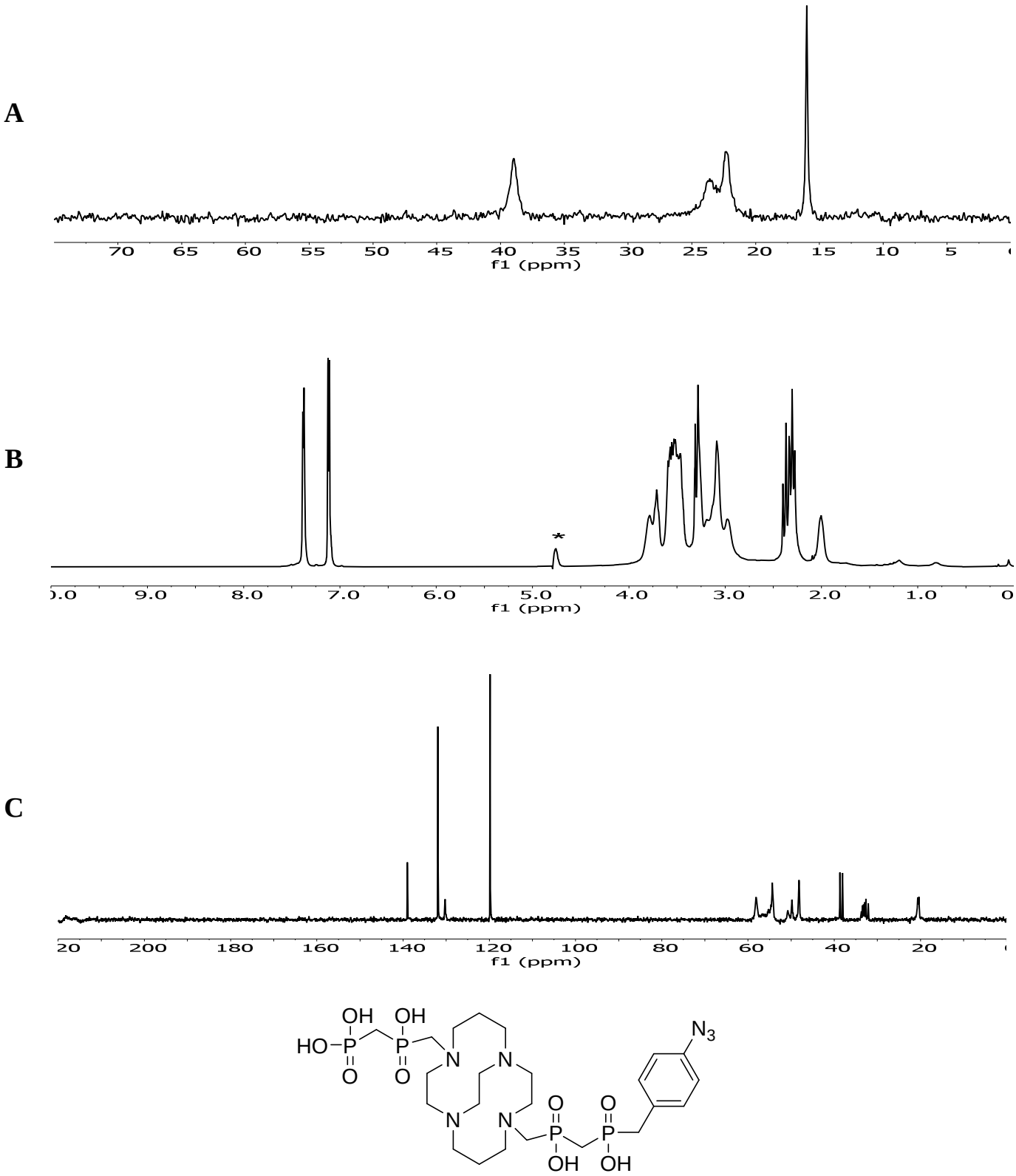

Figure S28. Characterization $^{31}P\{^{1}H\}$ (**A**), ^{1}H (**B**) and $^{13}C\{^{1}H\}$ (**C**) NMR spectra of **21** in D_2O (pD ~3). Residual water signal after pre-saturation in **B** (around 4.8 ppm, labelled *) was removed for clarity reasons. Signals of *t*-BuOH were labelled *.

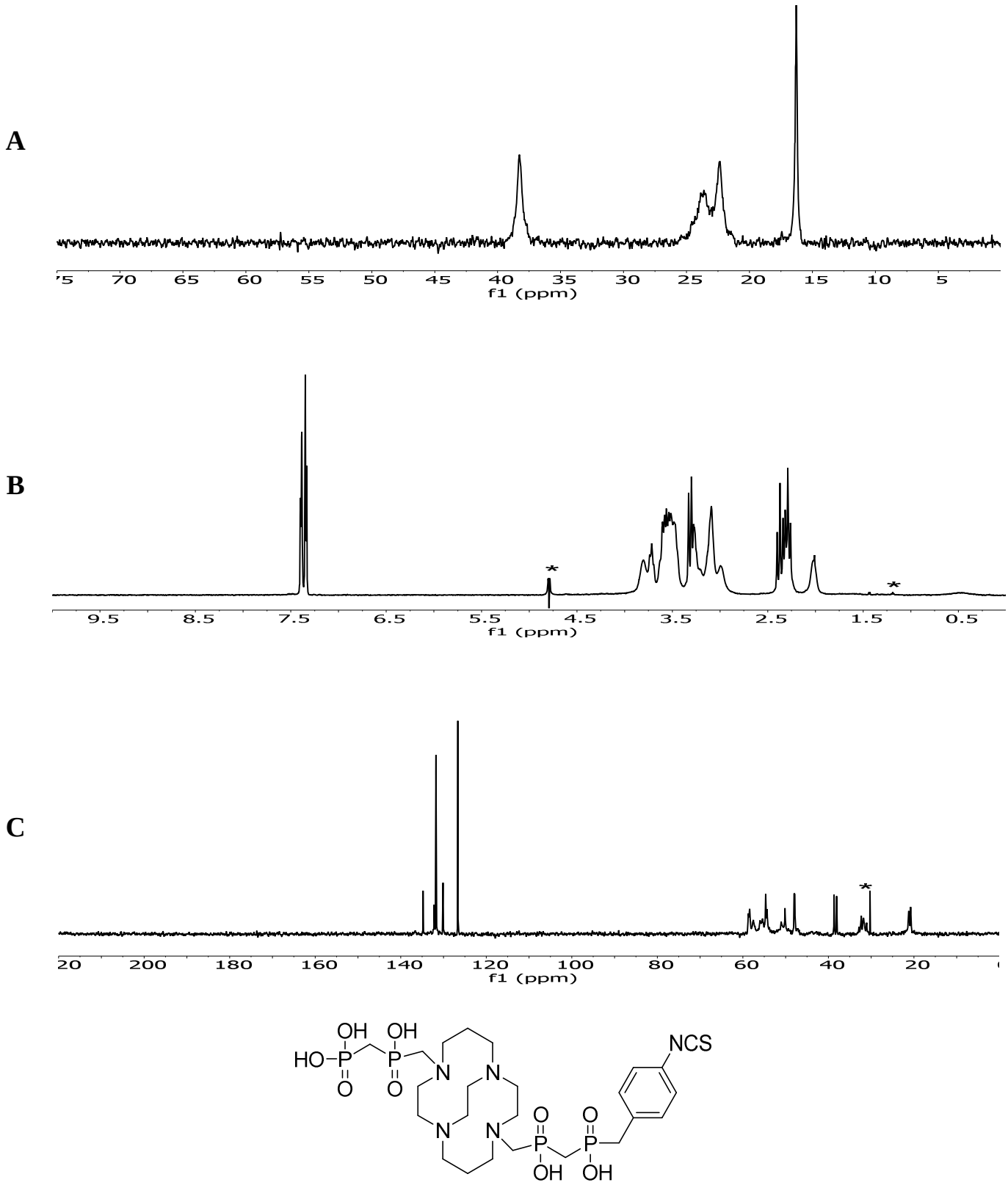

Figure S29. Characterization $^{31}P\{^{1}H\}$ (**A**), ^{1}H (**B**) and $^{13}C\{^{1}H\}$ (**C**) NMR spectra of **22** (purity >95 %) in D_2O (pD < 1). Signals of *t*-BuOH were labelled *.

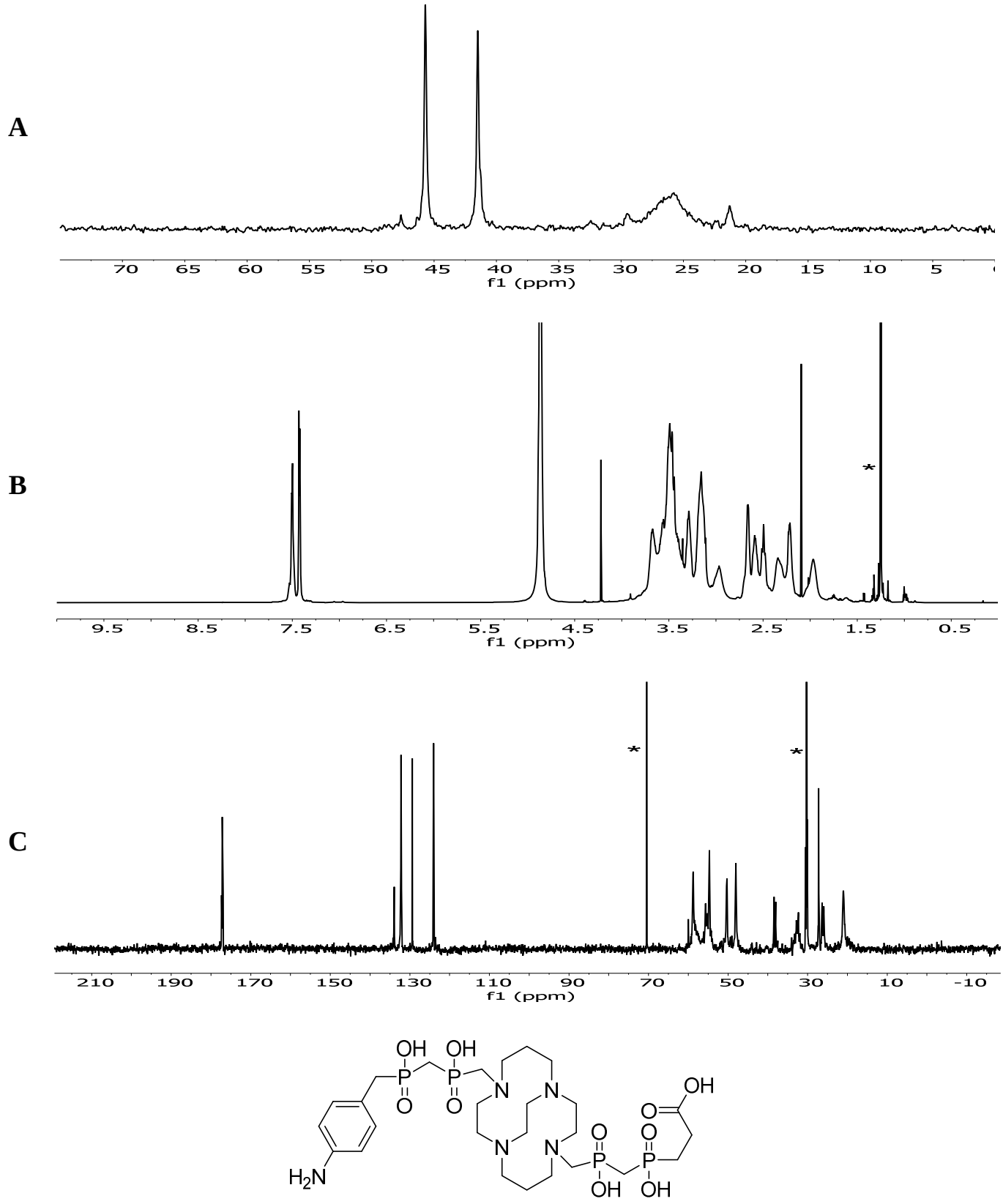

Figure S30. Characterization $^{31}P\{^{1}H\}$ (**A**), ^{1}H (**B**) and $^{13}C\{^{1}H\}$ (**C**) NMR spectra of **23** in D_2O (pD ~1.6). Residual signals of TFA in **C** are labelled *. Signals of *t*-BuOH were labelled *.

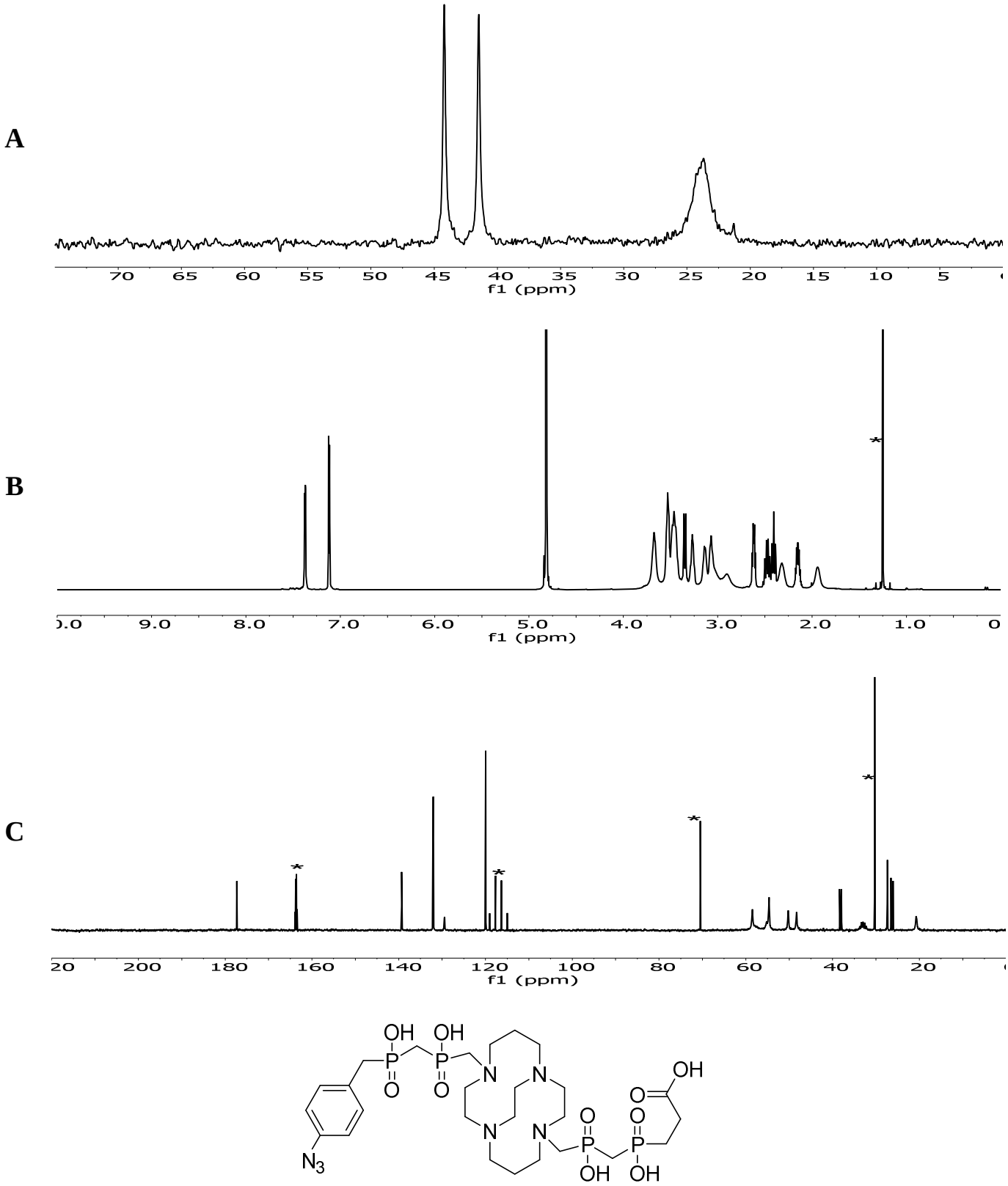

Figure S31. Characterization $^{31}P\{^{1}H\}$ (**A**), ^{1}H (**B**) and $^{13}C\{^{1}H\}$ (**C**) NMR spectra of **24** (purity of ~90 %, according to ^{31}P NMR) in D_2O (pD ~7.2). Residual solvents in **B**, TFA signals in **C** and impurities in **A** are labelled *. Signals of *t*-BuOH were labelled *.

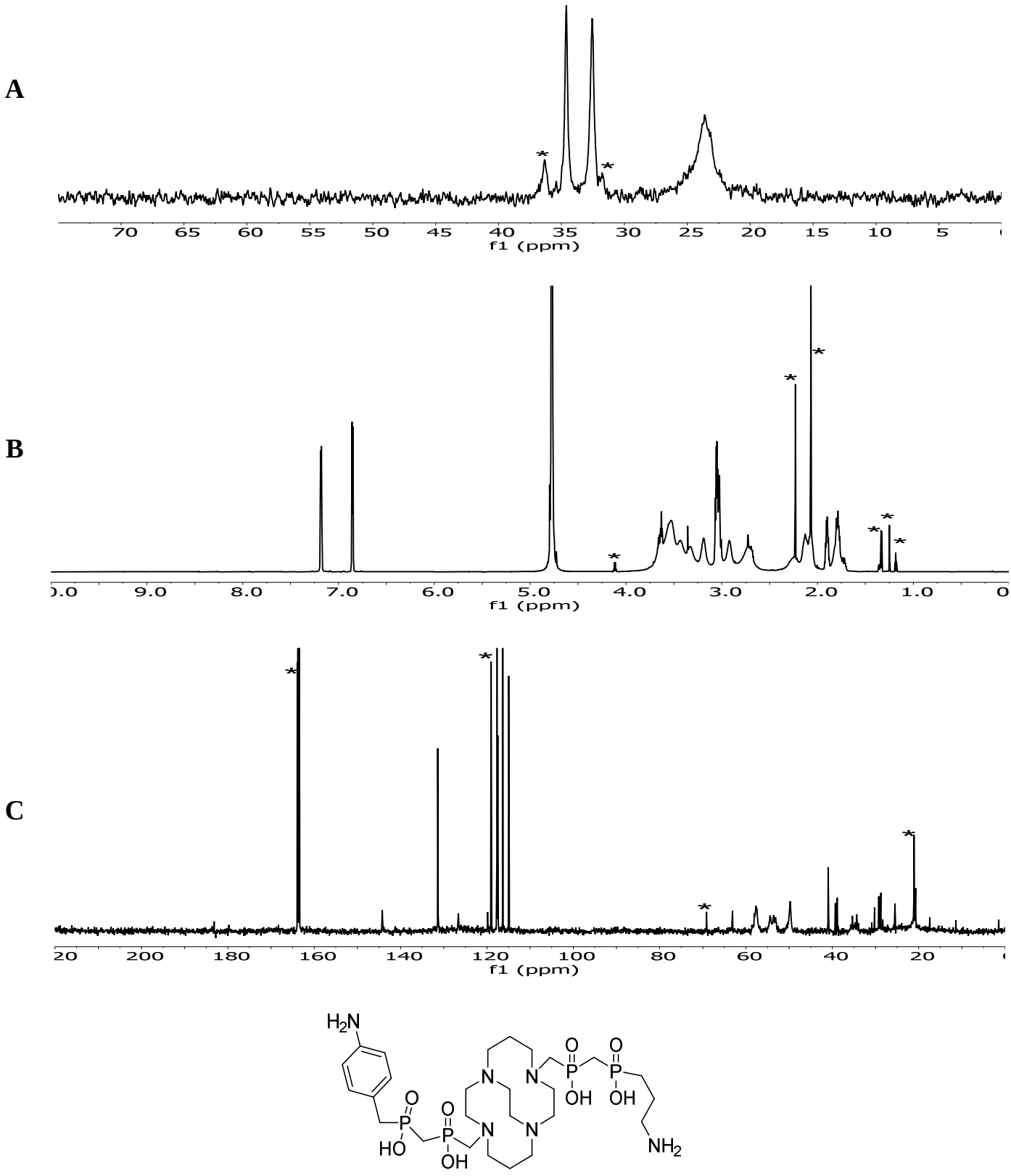

Figure S32. Characterization $^{31}P\{^{1}H\}$ (**A**), ^{1}H (**B**) and $^{13}C\{^{1}H\}$ (**C**) NMR tetrazine compound **25** in D_2O (pD ~3.0). Residual signal after water pre-saturation in **B** (around 4.8 ppm, labelled *) was removed for clarity reasons.

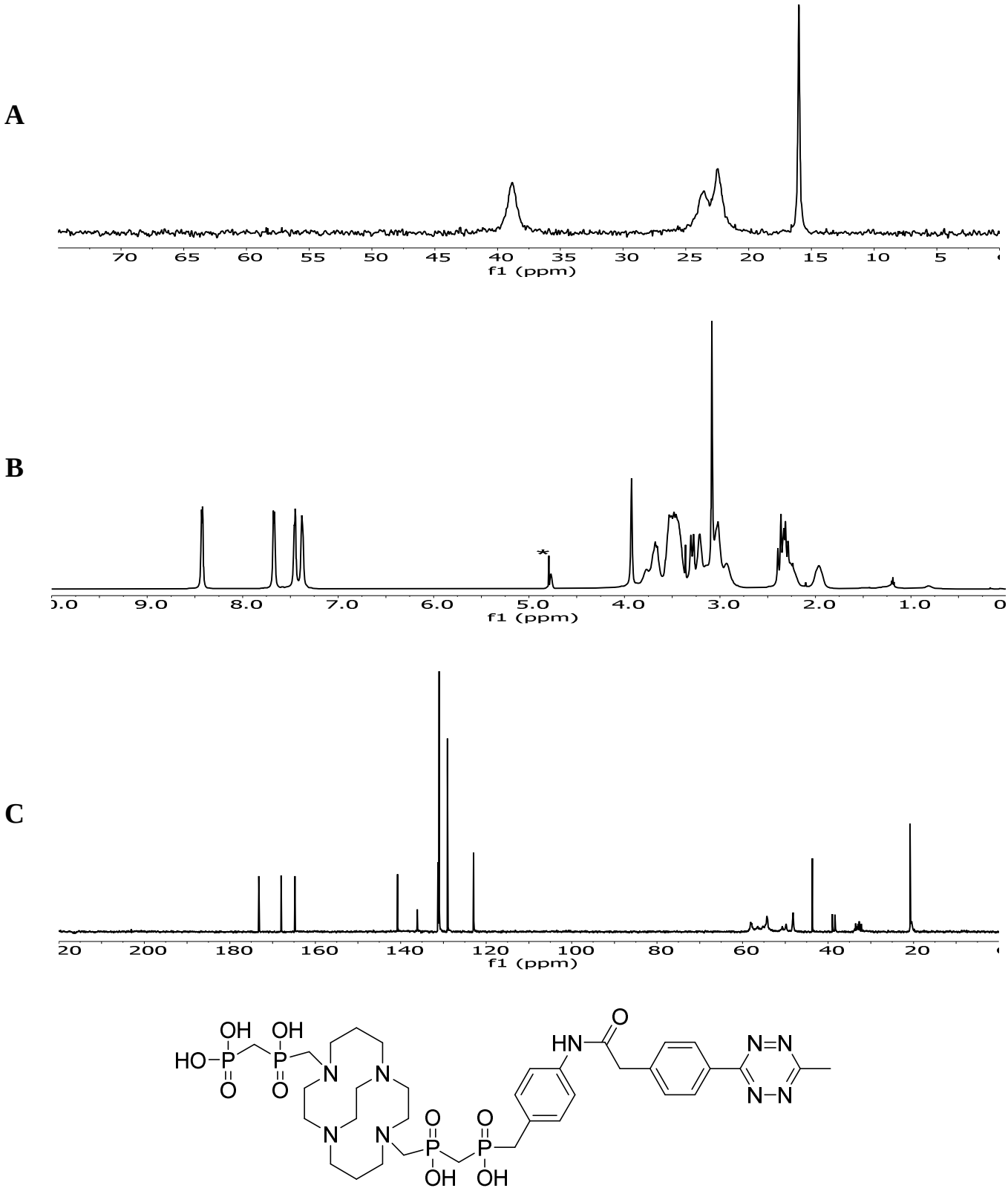

Figure 33. Characterization $^{31}P\{^{1}H\}$ (**A**), ^{1}H (**B**) and $^{13}C\{^{1}H\}$ (**C**) NMR spectra of compound **26** in D_2O (pD ~2). Residual solvents in **B**, and TFA signals in **C** are labelled *. Signals of *t*-BuOH were labelled *.

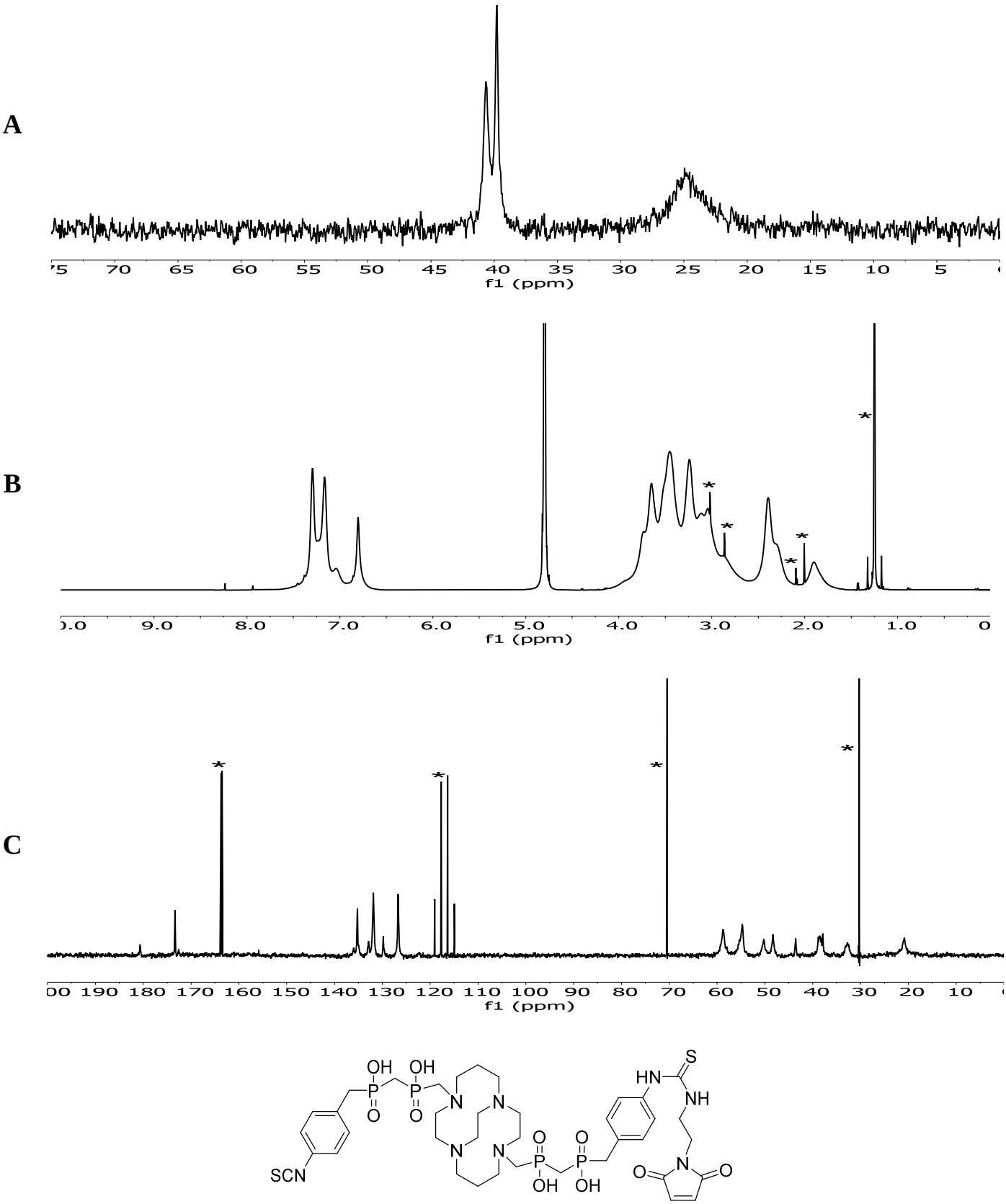

Figure 34. Characterization $^{31}P\{^{1}H\}$ (**A**), ^{1}H (**B**) and $^{13}C\{^{1}H\}$ (**C**) NMR spectra of compound **26a** in D_2O (pD ~2). Residual solvents in **B**, and TFA signals in **C** are labelled *. Signals of *t*-BuOH were labelled *.